

Polyphosphate in Marine Environments and  
*Beggiatoa* sp. – Quantification and Visualization

**Dissertation**

zur

Erlangung des akademischen Grades

*Doctor rerum naturalium* (Dr. rer. nat.)

der Mathematisch-Naturwissenschaftlichen Fakultät

der Universität Rostock

vorgelegt von

Simon Langer

Rostock, August 2019



Tag der Einreichung: 23.08.2019

Tag der Verteidigung: 01.11.2019

1. GutachterIn:

Prof. Dr. Heide Schulz-Vogt  
Leibniz-Institut für Ostseeforschung Warnemünde  
Geomikrobiologie

2. GutachterIn:

PD Dr. Stefan Forster  
Universität Rostock  
Meeresbiologie



## Table of content

<b>Zusammenfassung</b>	<b>III</b>
<b>Summary</b>	<b>1</b>
<b>1 Introduction</b>	<b>3</b>
1.1 Microbial phosphorus cycling .....	3
1.2 Polyphosphate .....	4
1.3 Polyphosphate habitats .....	6
1.4 Challenges in (poly)P research.....	7
1.5 Aims of this thesis .....	9
<b>2 Material and Methods</b>	<b>11</b>
2.1 Study areas .....	11
2.1.1 Hütelmoor and Baltic Sea .....	11
2.1.2 Upwelling and oxygen minimum zone off Peru .....	11
2.2 Sampling.....	12
2.2.1 Sampling in the Study site of Baltic Trancoast: Hütelmoor and Baltic Sea .....	12
2.2.2 Sampling oxygen minimum zon off Peru .....	13
2.3 Processing of sediments and filament analysis .....	14
2.3.1 Counting/ picking of filaments .....	14
2.3.2 Light-/ fluorescent microscopy .....	14
2.3. Polyphosphate quantification .....	14
2.4 Experiments for nanoSIMS .....	15
2.4.1 Lab experiments.....	15
2.4.2 Ex situ incubations of sediment cores from the Peruvian upwelling area .....	18
<b>3 Results</b>	<b>19</b>
3.1 PolyP quantities in different environments .....	19
3.1.1 PolyP in a coastal zone of the Baltic Sea .....	19
3.1.2 PolyP in the pelagic zones at two stations off Peru .....	21
3.2 PolyP in <i>Beggiatoa</i> off Peru.....	22
3.2.1 Qualitative analyses of polyP (Microscopy).....	22

3.2.2	Number, diameter distribution and biovolume of <i>Beggiatoa</i> filaments from the continental shelf off Peru.....	23
3.2.3	Quantitative analyses of polyP in <i>Beggiatoa</i> .....	26
3.3	NanoSIMS results.....	27
3.3.1	Phosphorus and <sup>18</sup> O distribution in <i>Beggiatoa</i> sp. 35Flor after in situ incubations.....	27
3.3.2	Differences between defined regions of interest (ROIs).....	30
3.3.3	Sulfur distribution in <i>Beggiatoa</i> sp. filaments after in situ incubations .....	33
3.3.4	Ex situ incubations of sediment cores from the Peruvian upwelling.....	35
<b>4</b>	<b>Discussion</b>	<b>37</b>
4.1	Quantities and relevance of polyP in coastal and marine environments .....	37
4.1.1	PolyP in a coastal area of the Baltic Sea.....	37
4.1.2	PolyP in the pelagic zone off Peru .....	40
4.2	Contribution of biologically stored polyP to sedimentary P fluxes .....	41
4.2.1	Filamentous Sulfur bacteria in Peruvian upwelling areas.....	41
4.2.2	Presence and size of polyP inclusion in filamentous sulfur bacteria .....	42
4.2.3	Contribution of PolyP storage to sedimentary phosphate release.....	43
4.3	Visualization of an active intracellular polyP pool .....	48
<b>5</b>	<b>Conclusion and Outlook</b>	<b>55</b>
	<b>References</b>	<b>57</b>
	<b>List of Figures</b>	<b>68</b>
	<b>List of Tables</b>	<b>71</b>
	<b>Acknowledgment</b>	<b>72</b>
	<b>Declaration of Authorship</b>	<b>73</b>

## Zusammenfassung

Polyphosphat wurde in den letzten Jahren zunehmend als wichtiger Bestandteil des mikrobiellen Phosphorkreislaufs wahrgenommen, insbesondere bei wechselnden Redoxbedingungen. Dies beruht unter anderem auf seinen Phosphor- und energiereichen Eigenschaften, welche in verschiedenen Umgebungen und für Mikroorganismen von hoher Relevanz sind. Dennoch gibt es bis jetzt eine vergleichsweise geringe Anzahl an wissenschaftlichen Studien, welche sich auf die Rolle von polyP konzentrieren, überwiegend begründet in methodischen Schwierigkeiten. Diese Arbeit hat zum Ziel 1.) durch die Quantifizierung von polyP Einblicke in die saisonalen und räumlichen Verteilungsmuster in Küstengebieten zu erhalten, 2.) den möglichen Beitrag von filamentösen Schwefelbakterien zu Phosphatflüssen aus Sedimenten vor Peru zu bestimmen und 3.) eine neue Methode zu etablieren, welche die Visualisierung der Aktivität polyP relevanter Enzyme ermöglicht.

Während unregelmäßiger Probenintervalle im Laufe eines Jahres ergaben sich unterschiedliche Verteilungsmuster der polyP Konzentrationen, welche nicht mit unterseeischen Grundwasseraustritten des angrenzenden Küstengebietes in Verbindung gebracht werden konnte. So konnte lediglich eine geringe Relevanz von polyP auf den lokalen Phosphorkreislauf festgestellt werden. Dennoch konnte in allen Proben zu jeder Jahreszeit polyP nachgewiesen werden. Dies demonstriert das Vorhandensein eines permanenten zellulären polyP Pools, welcher möglicherweise der Aufrechterhaltung grundlegender Stoffwechselprozesse dient. Gleichbleibende polyP Konzentrationen wurden auch in filamentösen Schwefelbakterien aus Sedimenten vor Peru in unterschiedlichen Tiefen nachgewiesen. Es konnte gezeigt werden, dass schmale Filamente die der Gattung *Beggiatoa* zugeordnet wurden, einzelne große polyP Einschlüsse pro Zelle enthielten, die einen Durchmesser von bis zu 3  $\mu\text{m}$  erreichten und die größten bisher in Umweltproben gefundenen polyP Einschlüsse darstellen. Im Gegensatz dazu enthielten Filamente mit breiterem Durchmesser mehrere kleine polyP Einschlüsse, was auf unterschiedliche PolyP Akkumulationsmechanismen zwischen verschiedenen Arten innerhalb der Gattung *Beggiatoa* hindeutet. Das Vorhandensein von PolyP in *Beggiatoa* spp. unterstützt die Möglichkeit eines biologisch induzierten Beitrags zu ehemals beschriebenen Phosphatflüssen aus Sedimenten vor Peru. Die Aktivität des intrazellulären polyP Pool konnte durch eine neue Methode gezeigt werden, welche mit dem Modellorganismus *Beggiatoa* sp. 35Flor etabliert wurde. Diese basiert auf dem enzymatisch vermittelten Austausch von Sauerstoff in Wasser und Sauerstoff in Phosphat nach Zugabe von  $^{18}\text{O}$

markiertem Wasser. Starke  $^{18}\text{O}$  Anreicherungen wurden sowohl nach oxischen und anoxischen, sowie sulfidarmen und sulfidreichen Inkubationsbedingungen nachgewiesen. Die grundlegende metabolische Aktivität war bei anoxischen und sulfidreichen Bedingungen zugunsten der Aktivität von polyP assoziierten Enzymen eingeschränkt, was die zentrale Rolle von polyP bei ungünstigen Umweltbedingungen unterstreicht. Darüber hinaus deutet die konstante Aktivität polyP assoziierter Enzyme während günstigen Wachstumsbedingungen auf ein permanentes intrazelluläres Recycling von polyP hin, was die weit verbreitete Sichtweise auf polyP als inaktiver Phosphor und Energieträger während vorteilhafter Wachstumsbedingungen in Frage stellt.



## Summary

Polyphosphate has been increasingly recognized in recent years to represent an important component of the microbial phosphorus cycle, especially when oscillating redox conditions prevail. This is, among other things, predominantly based in its potential to serve as an additional phosphorus source in various environments and as an energy carrier being relevant for microorganisms. However, studies focusing on polyP are still lacking, preliminary reasoned in methodological difficulties. This thesis aimed to 1.) quantify polyP in coastal environments to get insights on its seasonal and spatial distribution patterns, 2.) asses the possible contribution of filamentous sulfur bacteria to sedimentary phosphate fluxes reported earlier off Peru and 3.) establish a novel method to visualize enzymatic activity of polyP related enzymes.

PolyP concentrations of bottom waters measured in irregular sampling intervals during one year revealed highly variable distribution patterns, which could not be linked to potential intrusions of submarine groundwater from the adjacent coast. Thus, a minor relevance of polyP to the local P budget was determined but polyP was nevertheless present in all samples during all times of the year. This demonstrates a permanent background level of polyP possibly for the maintenance of basic metabolic processes like synthesis of ATP. A constant level of polyP concentrations were also found in filaments attributed to the genus *Beggiatoa* sampled in sediments off Peru. Single large scaled polyP inclusions were determined in cells with small filament diameter, which reached up to 3  $\mu\text{m}$  in diameter representing the biggest polyP granules found so far in environmental samples. In contrast to this, filaments with bigger filament diameter contained several small polyP inclusions, which argues for different polyP accumulation mechanisms between different species within the genus *Beggiatoa*. The presence of polyP in *Beggiatoa* supports the possibility for a biological mediated contribution to sedimentary phosphate fluxes off Peru. This intracellular phosphorous pool was shown to be active demonstrated by a new method established in laboratory studies with the model organisms *Beggiatoa* sp. 35Flor. The fast exchange between oxygen phosphate and oxygen from water was used to label the intracellular enzymatic activity at polyphosphate. Strong  $^{18}\text{O}$  enrichments were found after both oxic and anoxic and low and high sulfide incubation conditions. A focus of enzymatic activity at polyP during unfavorable growth conditions at the expense of standard metabolic processes was determined underlining the pivotal role of polyP during stressful environmental conditions. Furthermore, a constant activity of polyP

related enzymes was also determined during favorable growth conditions, which argues for a permanent recycling of polyP challenging the widespread view of polyP as an inactive phosphorus and energy carrier during non-stressful growth conditions.

## 1 Introduction

### 1.1 Microbial phosphorus cycling

Phosphorus (P), the 13<sup>th</sup> element described (Emsley, 2001), is one of the most important element for life and P molecules are essential functional and structural components of all organisms (Paytan & McLaughlin, 2007). They provide cell structure and cell compartmentalization through the formation of phospholipids, phosphoesters form the backbone of DNA/RNA, P molecules are indispensable for the storage and expression of genetic information and adenosine triphosphate (ATP) provides energy through phosphoanhydride bonds. Furthermore, P has many metabolic regulatory functions, for example through phosphorylation and dephosphorylation of proteins. P compounds thus play an important role for microbial life and are present in a variety of inorganic and organic forms in dissolved and particulate pools, which is referred to as the microbial P cycle (Karl, 2014). The most prominent and typically used P molecule for microbial cells is inorganic phosphate ( $P_i$ ) and its derivatives. The basic processes associated with this molecule are depicted in Figure 1 (after Blake et al., 2005).

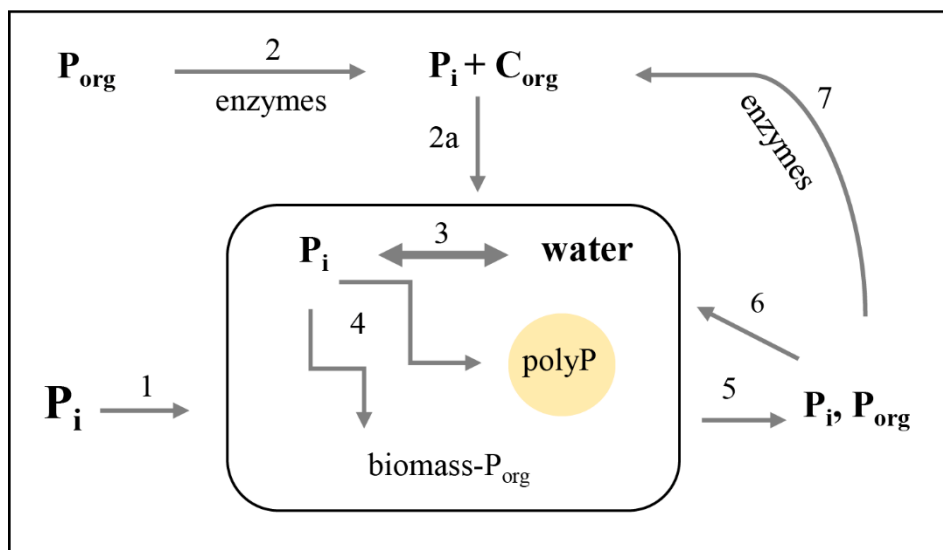


**Figure 1:** Phosphate cycling in bacteria in aquatic environments. Dissolved  $P_i$  can be taken up by free diffusion (1) or via membrane bound transport proteins (2a) after enzymatic mediated extracellular hydrolysis of organic P compounds (2).  $P_i$  in the cytoplasm is subjected to an array of enzymatic processes leading to oxygen isotope exchange between water and phosphate (3), before it is incorporated into inorganic (e.g. polyphosphate) or organic (e.g. biomass) compounds (4). Metabolic processes or cell dead/ lysis lead to the release of intracellular P compounds (5), which can be taken up again ( $P_i$ , 6) or recycled through extracellular enzymes ( $P_{org}$ , 7). (Figure and content of description after Blake et al., 2005).

As noted above, P typically occurs in its fully oxidized form and has long been regarded to be constrained in respect to biogeochemical redox cycling, when compared to the cycling of C, N or S compounds. However, this has changed in recent years since reduced P compounds like phosphite and hypophosphite were found to be used by microbes for energy metabolism (Schink & Friedrich, 2000; Stone & White, 2012). In addition, less oxidized varieties of P compounds such as phosphonate and phosphite have been found to be present in diverse environments (Hanrahan et al., 2005; White & Metcalf, 2007) and it is estimated that around 10% of all dissolved P in the ocean has a lower redox state than  $P_i$  (Pasek et al., 2014). Altogether, this hints to the presence of a biologically mediated redox cycle, which is further assumed to be a common part of the microbial P cycle (Karl, 2014) and highlight the necessity of intensified P research. This is also true for polyphosphate (polyP), another inorganic molecule with fully oxidized P atoms, which has been regarded as “a largely forgotten molecule” (Kornberg et al., 1995), but went to “prominent again in the marine P-cycle” (Björkman, 2014)

## 1.2 Polyphosphate

Inorganic polyphosphates are linear molecules, which consist of tens to hundreds of phosphate residues being linked by high energetic phosphoanhydride bonds (Figure 2, Yoshida, 1954; Thilo, 1955; Kornberg & Ault-Riché, 1999).

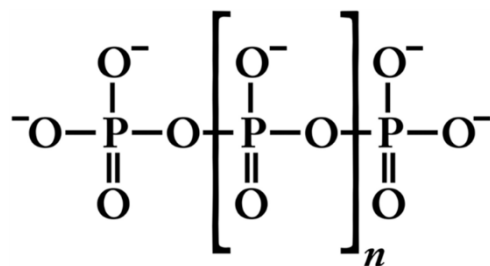


**Figure 2:** Linear polyP with variable length (n).

The molecule was first isolated from yeast more than 130 years ago as cyclic metaphosphoric acid (Liebermann, 1888) and first described as volutin granules by Meyer in 1904. It has been argued that polyP was present and produced on a large scale in the prebiotic world (Yamagata

et al., 1991), where it is assumed to have played a key role in the origin of life (Brown & Kornberg, 2004, Achbergova & Nahalka, 2011). This is supported by the presence of polyP in all three domains of life and the often highly conserved enzymes being involved in polyP cycling (Rao et al., 2009; Zhang et al., 2002). Two of the most important enzymes related to polyP metabolism are polyphosphatekinases (PPK) and exopolyphosphatases (PPX) (Kulaev & Kulakovskaya, 2000). The formation of polyP is predominantly mediated by the catalytic activity of PPK, which cleaves the terminal  $\gamma$ -P<sub>i</sub> from nucleotidtriphosphate (NTP) to prolong or synthesize new polyP chains (Kornberg et al., 1956; Reaction 1).



A differentiation between PPK1 and PPK2, which differ in their substrate preference (reaction 1 + 2), was made 2002 by Zhang et al. PPK1 exclusively uses ATP as a phosphate donor for synthesis of polyP (reaction 2) being 4 fold faster than the reverse reaction at 37 °C (Ishige et al., 2002), which breaks down polyP and thus reducing polyP chain lengths.



In addition, utilization of polyP for phosphorylation of nucleoside diphosphate is not specific, but favors adenosine diphosphate (ADP) with a 30 fold preference over guanosine diphosphate (GDP) (Ishige et al., 2002), followed by uridine diphosphate (UDP) and cytidine diphosphate (CDP) (Kuroda & Kornberg, 1997). PPK2 in contrast favors GDP over ADP for the breakdown of polyP and can use both ATP and guanosine triphosphate (GTP) for the synthesis of polyP (Ishige et al., 2002).



The breakdown of polyP with concomitant phosphorylation of GDP to GTP is 75 fold faster than the synthesis of polyP from GTP at 37 °C (Ishige et al., 2002) suggesting that PPK2 is predominantly involved in polyP degradation, whereas PPK1 is mainly responsible for polyP formation. Another enzymes involved in polyP degradation is the hydrolase PPX with concomitant release of P<sub>i</sub> from the ends of polyP (Akiyama et al., 1993, reaction 4)



This enzymatic activity is highly processive (Kornberg et al., 1999) and removes one P<sub>i</sub> residue after another from the ends of the polyP chain.

The ubiquitous presence of polyP together with the highly conserved enzymes are linked to an array of cellular functions attributed to this molecule. One example is the substitution of ATP as a  $P_i$  donor for phosphorylation processes (Kornberg, 1995), which has been observed in connection of phosphorylation of glucose (Szymona & Ostrowski, 1964) or proteins (Skorko, 1989). Furthermore, polyP provides an osmotic advantage compared to dissolved  $P_i$ , since the negatively charged polyanion is balanced by counter ions like  $Mg^{2+}$ , or  $Ca^{2+}$ . It is also supposed that it functions in molecular signaling and response to stressful condition (Kornberg, 1995).

### 1.3 Polyphosphate habitats

In addition to the ubiquitous presence and multitude functions of polyP, some organisms have the capability to accumulate extraordinary high amounts of  $P_i$  and store it as intracellular polyP. This uptake occurs through two proposed mechanisms: Luxury uptake and overplus response (Karl & Björkman, 2015). The latter mechanism was first observed in  $P_i$  starved yeast, which accumulated  $P_i$  when transferred from P poor to P rich medium and was later described as overplus response (Harold, 1964). It is assumed that this phenomenon is a common trait of microorganisms in oligotrophic systems, where  $P_i$  is readily depleted. This is supported by studies in these areas showing high abundances of genes involved in polyP metabolism (Temperton et al., 2011), increased polyP formation in *Trichodesmium* (Orchard et al., 2010) and preferred polyP storage resulting in higher polyP quotas compared to bulk P in phytoplankton (Martin et al., 2014). In contrast to this, algae and bacteria were also found to accumulate polyP with excess  $P_i$  available (Solorzano & Strickland, 1968), being referred to as “luxury uptake”, which is widely used in waste water treatment plants (e.g. McMahon & Read, 2013).  $P_i$  removal in these systems is achieved by oscillating between oxic and anoxic conditions, which is also an important environmental factor regulating polyP formation and degradation. This is well described for filamentous sulfur bacteria within the family *Beggiatoaceae*. One example are bacteria of the genus *Thiomargarita* sp., which were shown to induce hydroxyapatite formation by releasing  $P_i$  from intracellular polyP degradation (Schulz & Schulz, 2005). The model organism *Beggiatoa* sp. 35Flor was shown to degrade polyP with subsequent release of  $P_i$  into the environment (Brock & Schulz-Vogt, 2011), which is relevant in anoxic environments with high sulfate reduction rates and consequently pronounced sulfide production.

A redox sensitive release of  $P_i$  from lake sediments was already described several decades ago being implemented into a purely chemical model (Einsele 1936; Mortimer, 1941). In this model oxidized iron hydroxides, which have high absorption capacities for  $P_i$ , prevent the release of  $P_i$  to the overlaying water column. When these sediments become anoxic, the iron hydroxides are reduced and bound  $P_i$  is released. This is enhanced in organic rich sediments with high rates of sulfide reduction. Produced sulfide readily reduces iron hydroxides, which ultimately leads to the formation of iron sulfide (FeS) having a poor absorption capacity for P at neutral pH (Roden & Edmonds, 1997; Azzoni et al., 2005). However, the abiotic model was often found to not sufficiently explain the observed sedimentary  $P_i$  release leading to the assumption that microorganisms are directly involved in sedimentary P cycling (Davelaar 1993; Gächter and Meyer 1993). This was confirmed by several studies (e.g. Hupfer et al., 1995, Schulz & Schulz, 2005), but research about polyP lacks behind compared to other environmentally important compounds.

#### **1.4 Challenges in (poly)P research**

The in general limited amount of studies dealing with polyP in environmental samples is mainly associated with methodological difficulties in measuring polyP. Historically there are only limited attempts to measure polyP in seawater (Solorzano & Strickland, 1968), which used hydrochloric acid (HCL) to hydrolyze polyP with subsequent measurements of  $P_i$ . However, the high stability of phosphoanhydride bonds in polyP often leads to an underestimation of polyP. Hydrolysis by enzymatic action can be achieved by using PPX with subsequent measurement of  $P_i$  (Rao et al., 1998) or PPK for phosphorylation of ADP to ATP with  $P_i$  from polyP and subsequent ATP hydrolysis by luciferase with concomitant generation of light (Ault-Riché et al, 1998). Another technique is phosphorus-31 nuclear magnetic resonance ( $^{31}P$ -NMR), which has been used in an array of studies (Hupfer et al., 1995; Sannigrahi & Ingall, 2005; Diaz et al., 2008). This is particularly suited to make conclusions about bonding of P atoms in high molecular weight dissolved organic P, in which polyP is rarely present (Dhyrmann et al., 2007). In addition, a high sample volume is necessary for these analyses (Diaz et al., 2016) and is disadvantageous in many environments, since NMR does not measure polyP in aggregates or when complexed with metals (Kornberg et al., 1999). This insensitivity can lead to underestimations of polyP (Diaz & Ingall, 2010, Diaz et al., 2016).

More regularly used in recent years is the metachromatic effect of polyP when stained with a fluorescent dye shifting the emission to a higher wavelength (Stokes shift), which is also observed in other polyanions (Figure 3, Kornberg, 1995).

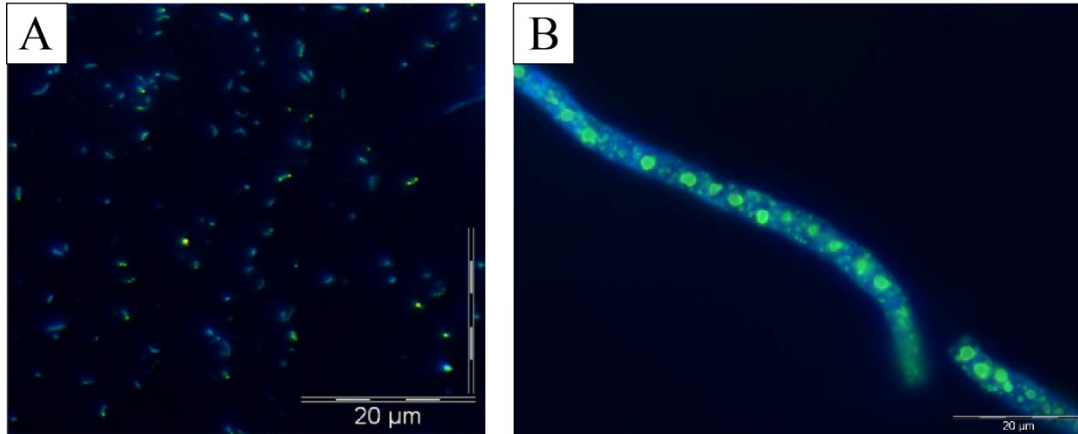


**Figure 3:** PolyP in bacteria stained with DAPI from an environmental sample (A) and in one *Beggiatoa* sp. 35Flor filament (B) discernible as yellow signals.

4',6-diamidino-2-phenylindole (DAPI) binds to both DNA and polyP. It was found that the emission spectrum is changed from 456 nm to 526 nm (excitation 360 nm) when DAPI is bound to polyP, hand in hand with a fluorescent signal being proportional to the concentration of polyP (Tijssen et al., 1982). This enables the quantification of high concentrations of polyP, because of the overlap between DAPI-DNA and DAPI-polyP emission spectra (Aschar-Sobbi et al., 2008). More sensitivity is achieved when DAPI is excited at 415 nm, which leads to an emission at 550 nm and thus to a better separation of DAPI-DNA and DAPI-PolyP (Aschar-Sobbi et al., 2008). The development of this fluorometric method has led to further insights about polyP in the environment and was used in this thesis.

The methodological challenges in polyP research are accompanied by general difficulties regarding P research, which are reasoned in the presence of only one stable P isotope. This limits studies being feasible with other elements with various stable isotopes like N or C, which are regularly used to track cellular activity and metabolites (Musat et al., 2012). Insights into microbial mediated P metabolism in aquatic and terrestrial environments also originates from studies using oxygen isotope ratios in  $P_i$  ( $\delta^{18}O_p$ ) (Paytan et al., 2002; Davies et al., 2014). The different  $^{18}O$  rations in  $P_i$  are caused by an enzyme mediated oxygen isotope exchange between oxygen-water and oxygen-phosphate. Pyrophosphatase (PPase) is the most dominant enzyme producing an equilibrium oxygen isotope effect within minutes and



is always involved during the incorporation of  $P_i$  into biomass regardless of the metabolic pathway (Cohn 1958; Blake et al., 2005). The application of  $^{18}O$  as an indirect tracer for P cycling will allow further insights into P metabolism of bacteria in environmental samples.

### 1.5 Aims of this thesis

The environmental role of polyP is often unclear, as methodological difficulties hampers insights into polyP metabolism. The focus of this PhD thesis was on achieving a better understanding of the relevance and occurrence of polyP in aquatic environments and allowing insights into its intracellular cycling. Methodological improvements based on the fluorescent method using DAPI were applied to quantify the polyP pool in environmental samples, which can potentially increase P loads in the environment. This was addressed in work package (WP) 1 with samples from the coastal zone of the Baltic Sea and from the pelagic zone at the continental shelf off Peru. The sediments present in the latter area were found to release large amounts of  $P_i$  exceeding P entering the sediment (Lomnitz et al., 2016). It has been hypothesized that filamentous sulfur bacteria of the family *Beggiatoaceae*, which regularly inhabit these sediments, might be responsible for this observation by degrading internally stored polyP with subsequent release of  $P_i$ . However, it has not been shown whether members of this family store polyP in this area and, therefore, have the potential to contribute to the sedimentary  $P_i$  fluxes. This was addressed in WP 2 aiming to study the abundance of filaments being responsible for polyP formation and to quantify the amount of polyP being stored. In addition, a new approach established in WP 3 was applied for these field samples to directly demonstrate polyP metabolism. For this purpose, a nanoSIMS method was established with the model organism *Beggiatoa* sp. 35Flor to allow a better understanding of polyP metabolism on a cellular level. It was hypothesized that incubation with  $^{18}O$ -water in combination with enzymatic activity leads to an enrichment of  $^{18}O$  in cellular structures, which in turn yields detailed insights also in polyP metabolism.

WP 1: Particulate polyP in a coastal area of the Baltic Sea and in the pelagic zone at the continental zone off Peru

- WP 2 Storage of polyP by marine *Beggiatoaceae* and their potential contribution to sedimentary phosphate fluxes
  
- WP 3 Visualization of enzymatically used polyP by establishing a new nanoSIMS approach

## **2 Material and Methods**

### **2.1 Study areas**

#### **2.1.1 Hütelmoor and Baltic Sea**

The Hütelmoor is located in the nature reserve “Heiligensee and Hütelmoor” being a coastal fen peat at the south-western coast of the Baltic Sea, northeast from Rostock. It developed between 5400 – 3900 years ago in the cause of the littorina sea transgression (Bohne & Bohne, 2008). Rising sea- and groundwater levels led to the formation of a coastal peatland, which was strongly connected to the Baltic Sea by regular flooding events. The Hütelmoor area was later subjected to an array of anthropogenic impacts starting from the 16<sup>th</sup> century (Bohne & Bohne, 2008). The construction of a dyke in 1903, which was rebuilt in 1963 (Miegel et al., 2016), was reasoned in strong erosions of the coast with up to 20 – 35 cm per year (Kolp, 1957) and advanced anthropogenic interests. This protected the village Markgrafenheide against water intrusions from the Hütelmoor, but permanently separated the peatland from the Baltic Sea, which led to a desalinisation of the area (Voigtländer et al., 1964, Bohne & Bohne, 2008). The maintenance of the coastal protection dune was stopped in the year 2000 in course of restoration measures to re-establish pristine conditions in the Hütelmoor area, which are characterized by periodical flooding with brackish water from the Baltic Sea. In addition, the area was flooded in 2009 and the development of the restoration measures have been monitored with foci on changing hydrological properties (Miegel et al., 2016) and effects on trace house gas emissions (Hahn et al., 2015). The connection between the Hütelmoor area and the Baltic Sea has been studied in the research project “Baltic Transcoast” with special emphasis on land-sea interactions like potential effects of submarine groundwater discharge (SGD).

#### **2.1.2 Upwelling and oxygen minimum zone off Peru**

One of the largest oxygen minimum zones (OMZs) in the ocean is present in the eastern tropical South Pacific Ocean within the Humboldt current upwelling system. Upwelling of nutrient rich waters at the Peruvian margin cause high primary production with up to 1.8 – 3.6 g C m<sup>-2</sup> (Strub & Mesías, 1998; Pennington et al., 2006). Together with bacterial respiration and the sinking of particulate organic matter in combination with sluggish ventilation, oxygen in this area is depleted and an extensive OMZ is formed (Karstensen et al., 2008, Kalvelage et al., 2015). The abundance of large sulfur bacteria of the family

*Beggiatoaceae* on the shelf has been repeatedly reported down to 300 m water depths (Arntz et al., 1991; Mosch et al., 2012, Sommer et al., 2016).

## 2.2 Sampling

### 2.2.1 Sampling in the Study site of Baltic Trancoast: Hütelmoor and Baltic Sea

Sampling spots in in the Hütelmoor area and the adjacent Baltic Sea are indicated in Figure 4. Samples for polyP quantification originated from groundwater in the Hütelmoor and from pore- and bottom water from the adjacent coast of the Baltic Sea. Groundwater from two wells was sampled in April, September and December 2016. 12 porewater samples for polyP quantification were obtained from six stations in summer 2016 and 20 bottom water samples were analyzed from 12 stations from the coastal Baltic Sea throughout the year 2016.

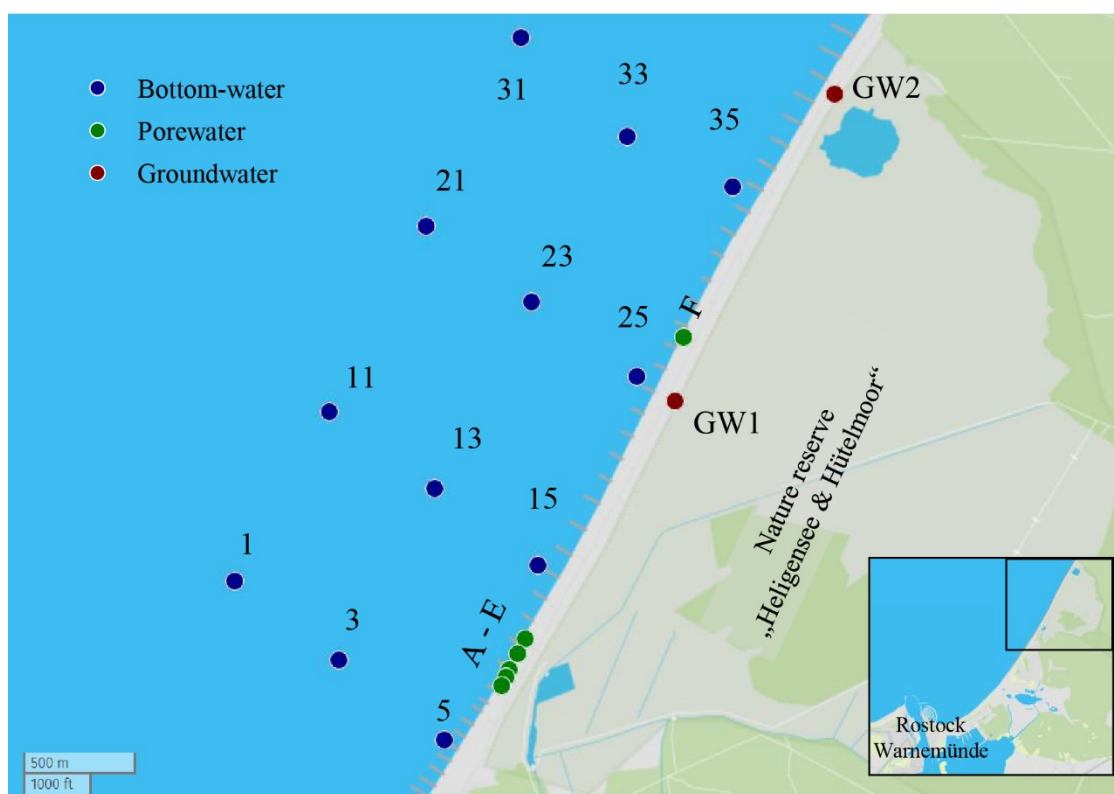


**Figure 4:** The study area of "Baltic Trancoast" with station numbers used for bottom-, ground-, and pore-water sampling for polyP quantification.

Bottom water samples were obtained in April, June, July, October and December from 12 stations in the coastal area of the Baltic Sea. Sampling was conducted with a Niskin bottle water sampler on board of the research boat "Klaashahn". Water was obtained as close to the seafloor as possible and filled into 1 L bottles, which were cooled until further processing

in the lab. Porewater was obtained with mobile “porewater lances” of 1 m length in summer 2016 from six different stations (A-F, Figure 4) along the coast of the Baltic Sea. Tips of the lances had openings of 500  $\mu\text{m}$  diameter. A stable aluminium pipe was inserted into the hollow lance and both were pushed into the maximum possible sediment depth. The inner tube was removed and porewater was obtained via a syringe attached to the sampling port from various depths while moving up. Groundwater samples were obtained from two groundwater wells installed in the Hütelmoor (GW1, GW2, Figure 4). Groundwater wells were placed either in peat or in sand layers. Sufficient volume for further analysis was only obtained from groundwater extracted from sandy sediments. The aged groundwater in the well was removed and fresh groundwater was collected and cooled until further processing in the lab. All water samples were filtered as soon as possible back in the lab through 0.22  $\mu\text{m}$  polycarbonate (PC) filters. Filters with particulate material were transferred to 2 ml Eppendorf cups and immediately frozen at  $-24\text{ }^{\circ}\text{C}$  until further analysis.

### 2.2.2 Sampling oxygen minimum zon off Peru

Water and sediment samples from the Peruvian shelf were obtained during the cruise M137 on the research vessel Meteor in May 2017 during austral fall in collaboration with the SFB754 of the Geomar, Kiel. Water samples for polyP quantification in the pelagic zone were sampled with Niskin bottles attached to a CTD from two stations with maximum water depths of 128 m ( $12^{\circ}16.79'\text{S } 77^{\circ}14.98'\text{W}$ ) and 244 m ( $12^{\circ}23.30'\text{S } 77^{\circ}24.28'\text{W}$ ). Water used for analyses originated from 10 m, 40 m, 100 m, 242 m (station 244 m total depth) and from 15 m, 30 m, 45 m, and 120 m (station 128 m total depth). 1L water was filtered in triplicates through 0.22  $\mu\text{m}$  PC filter directly after sampling. Filters were transferred to Eppendorf cups after filtration and were stored at  $-24\text{ }^{\circ}\text{C}$  until further processing back in the lab. Sediment cores for the analysis of *Beggiatoaceae* filaments were obtained with a multiple-corer (MUC) at 77 m ( $12^{\circ}13.50'\text{S } 77^{\circ}10.79'\text{W}$ ), 200 m ( $12^{\circ}08.00'\text{S } 77^{\circ}35.00'\text{W}$ ) and 244 m water depth. Subcores with 3.4 cm diameter and 30 cm length were immediately subsampled and stored at  $4\text{ }^{\circ}\text{C}$  for a maximum of 24 h.

### **2.3 Processing of sediments and filament analysis**

#### **2.3.1 Counting/ picking of filaments**

Sediments of the subcores were extruded within 24 h by gently pushing the sediment from the bottom end of the core with a matching cone. The top centimetre of the sediment was then transferred to a 50 ml centrifuge tube (Falcon) and filtered seawater was added to a final volume of 20 ml. The slurry, which contained  $\sim 9.08 \text{ cm}^3$  sediment, was gently mixed until a homogeneous mixture was achieved. Before filaments were picked and counted, 0.5 ml slurry, which contained  $\sim 0.227 \text{ cm}^3$  sediment, was pipetted into glass petri dishes containing filtered seawater. This suspension was inspected with a binocular and screened for filaments. Single filaments were picked with a self-made glass hook and transferred either onto glass slides or on PC filters. Filaments were picked and simultaneously counted from at least five 0.5 ml slurries until no further filaments could be identified. The numbers of filaments picked from  $0.277 \text{ cm}^3$  were used to calculate the total number of filaments per  $\text{cm}^3$  sediment. Triplicate filters with each 100 filaments were prepared from the three sampled depths for polyP quantification and frozen until analysis back in the lab.

#### **2.3.2 Light-/ fluorescent microscopy**

Filaments transferred on glass slides were immediately inspected with light microscopy to determine diameter and length of at least 150 filaments per depth. Filament diameter was measured with 400x magnification and filament length was measured with 100x magnifications using a calibrated ocular micrometer. Biovolumes of individual filaments and of all filaments per  $\text{cm}^3$  sediment were calculated assuming a cylindrical shape of the filaments. Filaments on PC filters were stained for 30 minutes with 3.61 mM DAPI solution to allow fluorescent microscopy for qualitative analysis of polyP granules at emission wavelength between 505 – 550 nm.

#### **2.3. Polyphosphate quantification**

Quantification of polyP was conducted based on protocols established by Aschar-Sobbi et al., 2008 and Martin & van Mooy, 2013 with modified buffer according to Kulakova et al., 2011. Filters in 2 ml Eppendorf cups were thawed at room temperature and 500  $\mu\text{l}$  TRIS buffer (20 mM, pH 7) was added. Filters were positioned at the inner side surface of the cups

if they were folded after adding the buffer. PolyP was extracted and brought into solution by adding one spatula glass beads (0.1 mm diameter) in combination with vigorous vortexing (Disrupter Genie, Scientific Industries) for 3 minutes with 2500 rpm. This was followed by a water bath at 100 °C for 5 min before samples were allowed to cool down on ice for 10 min. 100 µl subsample was transferred into new Eppendorf cups and 5 µl Mastermix composed of DNase (Riche Diagnostics GmbH) and RNase (Life Technologies) was added to each sample to purify the extract. Digestion proceeded for 10 min incubation at 37 °C with constant mixing at 300 rpm (Eppendorf Thermomixer Compact). Subsequently, 5 µl Proteinase K (Amresco, 100 µg per sample) was added and the previous digestion step was repeated. The cups were centrifuged at 10 000 x g (Eppendorf Mini-Spin-Plus) for 3 minutes and 100 µl of the supernatant was transferred into a well of a 96 microtiter plate (Omnilab). 5 µl of a 3.61 mM DAPI solution was pipetted on the side wall of each well followed by the addition of 200 µl buffer using a multi-pipette to assure a parallel start of the DAPI-polyP binding reaction. The plate was placed into a plate reader (TECAN infinite 200 PRO) and was mixed for 5 min at 452 rpm before the DAPI stained samples were excited at 415 nm and fluorescent emission at 550 nm was measured. Standards containing polyP-45 (chain length of 45 ± 5 phosphate residues) (Sigma-Aldrich) between 0.1 µM and 1.2 µM ran in parallel and were used to calculate absolute concentration of polyP in the original sample. Absolute concentrations of polyP were multiplied by 45 (= P<sub>i</sub> residues according to producer) to obtain PO<sub>4</sub><sup>3-</sup>- equivalents in polyP, which represent the maximum amount of substance phosphate being stored as polyP.

## 2.4 Experiments for nanoSIMS

### 2.4.1 Lab experiments

*The written parts of the following sections “H<sub>2</sub><sup>18</sup>O incubation of Beggiatoa sp. 35Flor”, “NanoSIMS analyses” and “statistical analysis” were published in the article “Simultaneous visualisation of enzymatic activity in the Cytoplasm and at Polyphosphate inclusions in Beggiatoa strain 35Flor incubated with <sup>18</sup>O- labeled water” in the journal “mSphere” on the 19<sup>th</sup> December 2018. I performed the experiments, did the data analysis and wrote all paragraphs”.*

### 2.4.1.1 H<sub>2</sub><sup>18</sup>O incubation of *Beggiatoa* sp. 35Flor

The strain *Beggiatoa* sp. 35Flor was cultivated in opposing gradients of oxygen and sulfide as described elsewhere in detail (Figure 5, Schwedt et al., 2012), with reduced phosphate concentrations of 20 μM leading to phosphate depletion within the mat after 7 days of growth (Brock & Schulz-Vogt, 2011).

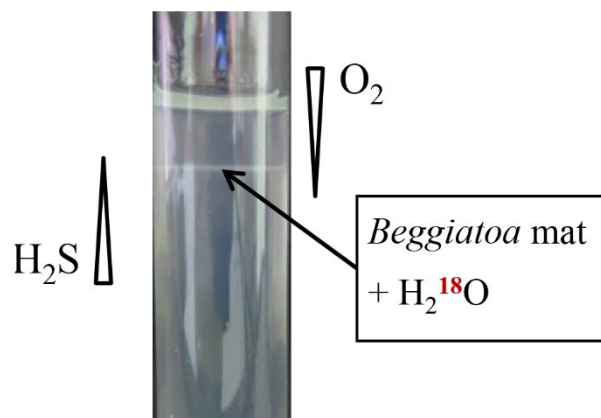


**Figure 5:** *Beggiatoa* filaments visible as a white mat situated at the oxic / anoxic interface between oxygen fluxes from the top and sulfide fluxes from the bottom. H<sub>2</sub><sup>18</sup>O was directly inoculated into the mat after 7 days of growth.

Sulfide concentrations in the bottom agar were 4 mM (low sulfide) and 24 mM (high sulfide). Seven days after inoculation of the medium, <sup>18</sup>O- water (97 atom% <sup>18</sup>O, Sigma Aldrich) was added to the mat of *Beggiatoa* filaments at the oxic-/ anoxic interface. Oxic treatments were incubated under continued micro-aerobic (oxic) conditions; anoxic incubation conditions were established by thoroughly replacing the atmosphere above the agar with N<sub>2</sub>. Control incubations were transferred to 4 °C after addition of <sup>18</sup>O-labeled water to reduce metabolic activity. Oxic and anoxic incubations were performed with both high and low sulfide concentrations in the bottom agar. The control incubation was conducted under oxic conditions with low sulfide concentration in the bottom agar. <sup>18</sup>O- water incubations proceeded for 24h, before single filaments were picked and transferred onto PC filters, which were stored at -24 °C until further processing.



**Table 1:** Conditions during 24 h incubation of *Beggiatoa* filaments with  $^{18}\text{O}$ - water.

	High $\text{H}_2\text{S}$	Low $\text{H}_2\text{S}$
Oxic	✓	✓
Anoxic	✓	✓
Control = Oxic; 4 °C	✓	✓

#### 2.4.1.2 NanoSIMS analyses

PC filters were thawed at room temperature and incubated with DAPI for at least 30 minutes. Subsequently cell integrity was visually confirmed by fluorescent microscopy using a LMD 6500 (Leica, Wetzlar, Germany, filter cube B/G/R). Positions of agar free filaments were marked with a laser pulse, which facilitated orientation for nanoSIMS analyses. The samples were coated with ca. 30 nm gold with a Cressington 108auto sputter coater (Watford, United Kingdom). NanoSIMS analyses were conducted at tagged positions with the simultaneously recording of images from the received secondary ions  $^{12}\text{C}^-$ ,  $^{16}\text{O}^-$ ,  $^{18}\text{O}^-$ , and  $^{31}\text{P}^-$  as described in Braun et al., 2018.

Data analysis was performed with the Look@NanoSIMS software (Polerecky et al., 2012). Previous to plane accumulation and drift correction, a maximum of three erroneous planes (with e.g. signal instabilities) were removed. Regions of interest (ROIs) were determined based on P counts normalized to C counts (P/C). P rich (redish spots) in contrast to P poor (bluish spots) were manually assigned as ROIs (Figure 15). Counts for each individual ROI were obtained for  $^{12}\text{C}^-$ ,  $^{31}\text{P}^-$ ,  $^{18}\text{O}^-$  and  $^{16}\text{O}^-$ , which were used to calculate C/P ratios and  $^{18}\text{O}$  enrichments in atom%.  $^{18}\text{O}$  enrichments were plotted against C/P (relative phosphorus content) to determine the threshold value between ROIs representing polyP and ROIs representing cytoplasm (Figure 16). The cutoff was set at a C/P ratio of 18 with ratios below 18 regarded as polyP (relatively high P content) in contrast to ratios above 18 (relatively low P content). This was based on the most pronounced gap in most treatments between adjacent ROIs. Significant differences between ROIs assigned as polyP versus ROIs assigned as cytoplasm based on C/P ratios were confirmed by statistical analyses (details below).

However, it is important to note that 18 is only the best suited value for this particular sample set, but not valid as a general cutoff. Since nanoSIMS does not give absolute values, individual cutoffs have to be defined for each individual study.

### **2.4.1.3 Statistical analysis**

The software “R” was used for statistical analyses. ROIs from filaments within the same treatment were pooled after confirming no significant differences between ROIs of filaments incubated under the same conditions based on counts of P,  $^{16}\text{O}$  and  $^{18}\text{O}$ . Significant differences in C/P ratios (indicative for P content) between ROIs defined as polyP and ROIs defined as cytoplasm were confirmed with the Whitney-U-Test. The non- parametric Kruskal- Wallis test followed by the Dunn’s test were performed to identify differences in  $^{18}\text{O}$  enrichments between the treatments, and between polyP granules and the cytoplasm.

### **2.4.2 Ex situ incubations of sediment cores from the Peruvian upwelling area**

#### **2.4.2.1 Description incubation setup**

Sediment cores from 200 m depth with in situ oxygen concentrations were incubated in an ex situ setup described in Dale, Roy et al., (unpublished) for 3.5 days. Samples from the overlying water column were obtained on a daily routine for nutrient analysis and ICP-OES. The sampled volume was replaced with bottom water from the 200 m site and nitrate and sulfide concentrations were monitored. Accumulation of sulfide was prevented by the regular addition of nitrate to the bottom water. After 7 days incubation, sulfide was allowed to accumulate and 9 ml  $^{18}\text{O}$ - water (Sigma Aldrich) was added into the overlying water leading to an isotopic enrichment of  $\sim 1$  atom%  $^{18}\text{O}$ . Incubation with  $^{18}\text{O}$  continued for 24 h before the core was sectioned. *Beggiatoaceae* filaments were picked from the upper centimeter and were transferred on PC filters, which were frozen for later nanoSIMS measurements as described in section 2.4.1.2.

#### **2.4.2.2 NanoSIMS analyses ex situ experiments**

Analyses of nanoSIMS results proceeded as described above and ROIs were defined based on P content. The threshold value for the differentiation between polyP and cytoplasm was set to a P/C ratio of 0.005.

### 3 Results

#### 3.1 PolyP quantities in different environments

##### 3.1.1 PolyP in a coastal zone of the Baltic Sea

PolyP was quantified in 20 bottom water samples, 16 porewater samples and 3 groundwater samples originating from the coastal zone of the Baltic Sea near the village Markgrafeneheide and the adjacent nature reserve “Heligensee und Hütelmoor”. Concentrations are presented as  $\text{PO}_4^{3-}$  equivalents ( $\text{P}_i$ -equiv.) in the measured polyP pool. Bottom water samples were obtained in April, June, July, October, and December and quantities of  $\text{P}_i$ -equiv. in polyP are presented in Figure 6.

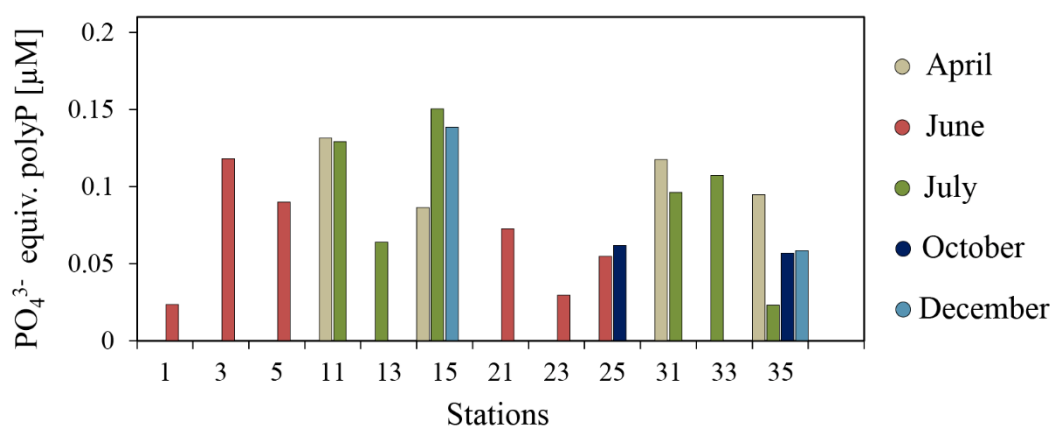


**Figure 6:** Concentrations of  $\text{P}_i$ -equiv. in polyP in bottom water samples at different stations during different months in 2016.

Highest concentrations with minor differences were measured in samples from July and December at station 15 with  $\text{P}_i$ -equiv. of  $0.16 \mu\text{M}$  and  $0.13 \mu\text{M}$ . 40% lower concentrations ( $0.09 \mu\text{M}$   $\text{P}_i$ -equiv.) were found in April at the same station. Lowest concentrations were found in June at stations 1 ( $0.02 \mu\text{M}$ ) and 23 ( $0.03 \mu\text{M}$ ), as well as in July at station 35 ( $0.02 \mu\text{M}$ ). Concentrations at the latter station were three times higher in October/ December ( $0.06 \mu\text{M}$ ) and five times higher in April ( $0.1 \mu\text{M}$ ) than the lowest concentration in July. PolyP concentrations in porewater samples were obtained from six stations at the beach and are shown in Figure 7.  $\text{P}_i$ -equiv. in polyP from porewaters were similar to bottom water samples at stations B, C and E (Figure 7 A). Concentrations at station C at 10 cm depth were similar to concentrations at station E at 25 cm and 50 cm depth with ca  $0.2 - 0.3 \mu\text{M}$   $\text{P}_i$ -equivalents.  $0.1 \mu\text{M}$  were measured at station B at 10 cm depth, which decreased to  $0.02 \mu\text{M}$

at 30 cm and 85 cm depth. Samples obtained from station A, D and F showed pronounced higher concentrations of  $P_i$ -equiv. (Figure 7 B). 0.25  $\mu\text{M}$  and 0.5  $\mu\text{M}$  were present at 30 cm depth at station A, 0.5  $\mu\text{M}$  at station F at 42 cm depth and highest concentrations were found at station D at 50 cm depth with 1.5 - 2  $\mu\text{M}$ .

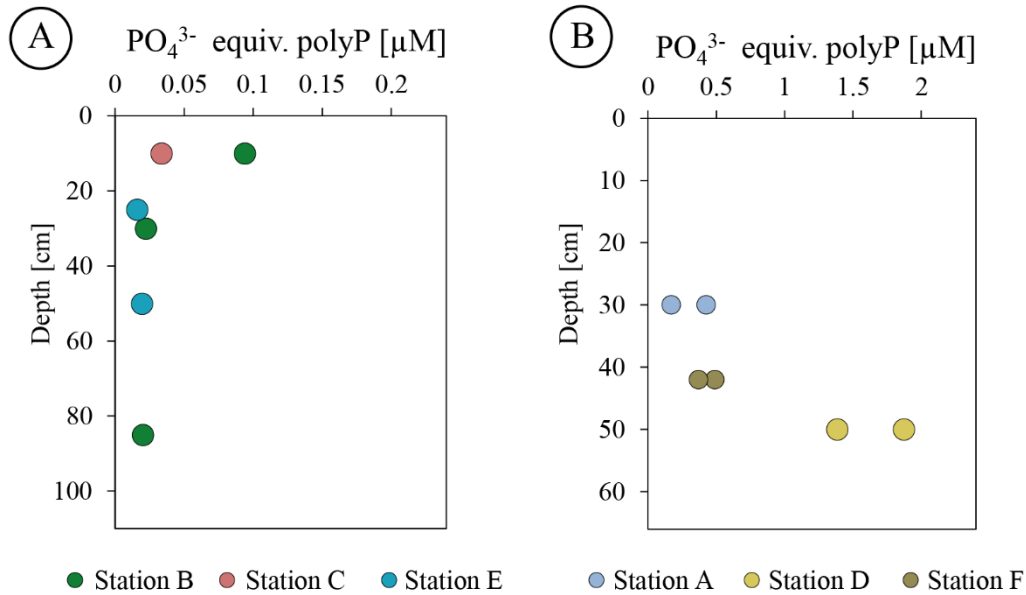


**Figure 7:** Concentrations of  $P_i$ -equiv. in polyP in porewater sampled at the beach.

PolyP concentrations in groundwater samples from station GW2 in the Hütelmoor were similar in April and September with ca. 0.3  $\mu\text{M}$   $P_i$ -equiv. and increased to 0.5  $\mu\text{M}$  in December. Groundwater from GW1 was measured in December and showed 0.1  $\mu\text{M}$   $P_i$ -equiv. in polyP (Figure 8).

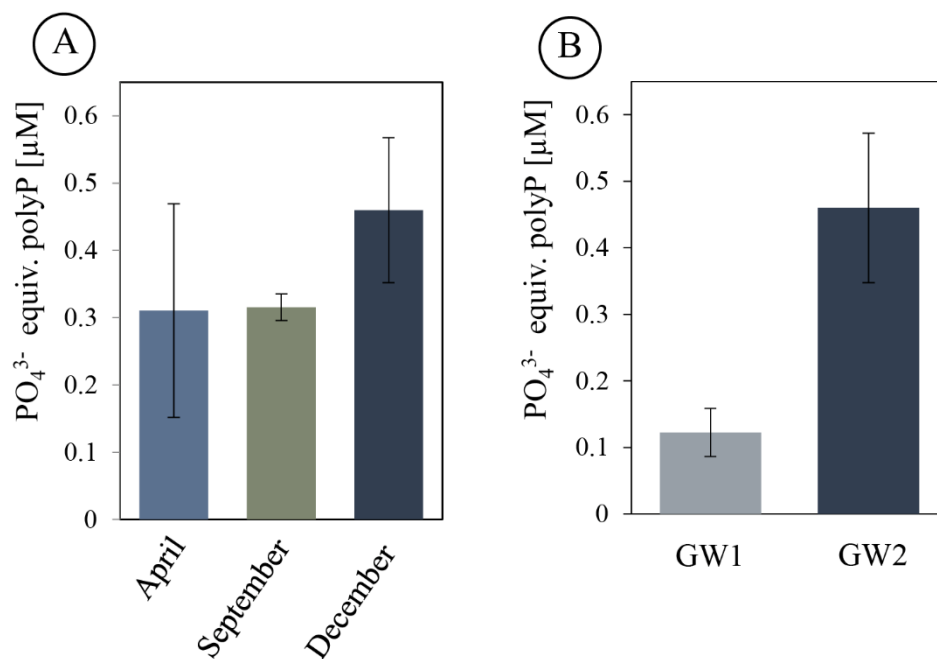


**Figure 8:** Mean Concentrations of  $\text{P}_i$ -equiv. in polyP in groundwater from two wells. GW2 was sampled in April, September and December (A). B shows concentrations sampled in December from both GW1 and GW2.

### 3.1.2 PolyP in the pelagic zones at two stations off Peru

PolyP in the pelagic zone was analyzed from two stations with maximum depths of 128 m and 244 m at the continental shelf off Peru.  $\text{P}_i$ -equiv. in polyP were relatively uniform at the shallower station with ca. 10 nM measured in 15 m, 30 m, 45 m and slightly decreased to 8.5 nM  $\text{P}_i$ -equiv. in 120 m depth (Figure 9 A). Similar concentrations between ~7 - 9 nM  $\text{P}_i$ -equiv. were measured at 40 m (9.2 nM), 100 m (6.8 nM) and 242 m depth at the station with a maximum depth of 244 m (Figure 9). Highest concentrations in the pelagic zone were present at the shallowest depth in 10 m with 20 nM.

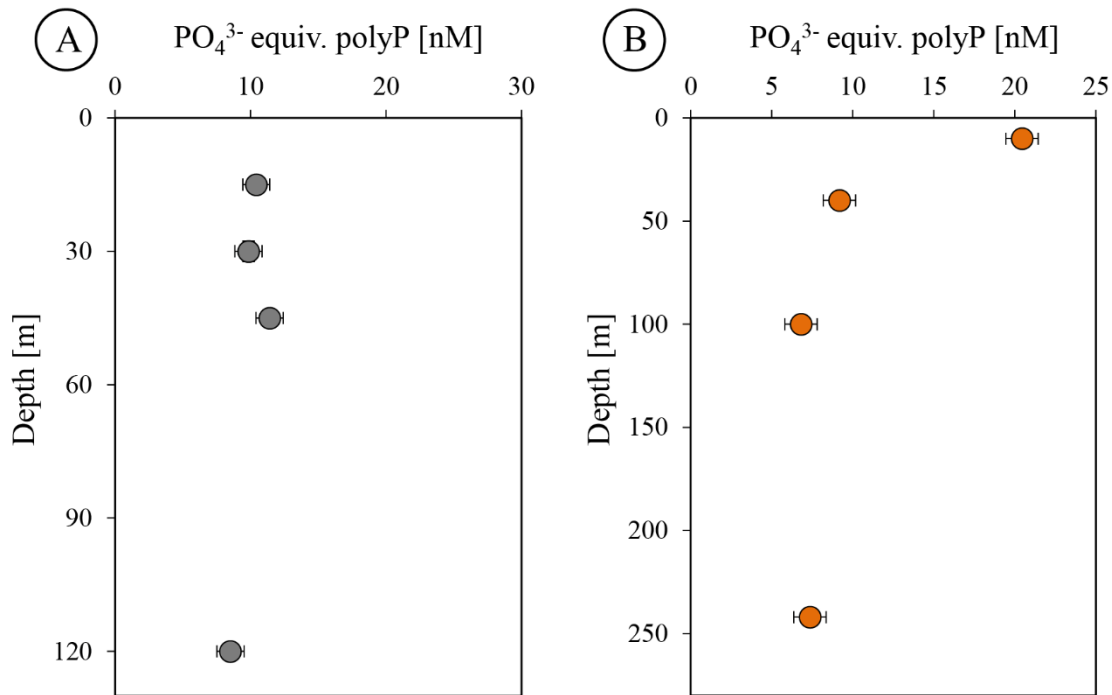


**Figure 9:** Means of  $\text{P}_i$ -equiv. in polyP in the pelagic zone of the continental shelf off Peru at stations situated at water depths of 128 m (A) and 244 m (B).

### 3.2 PolyP in *Beggiatoa* off Peru

#### 3.2.1 Qualitative analyses of polyP (Microscopy)

On board fluorescence microscopy did not show any evidence for polyP inclusions in DAPI stained bundles of *Marithioploca* and were not considered in the following. In contrast to this, polyP inclusions were present in filaments attributed to the family *Beggiatoaceae*. Diameters of polyP inclusions varied in size between 0.5  $\mu\text{m}$  and up to 3  $\mu\text{m}$  (Figure 10). The larger inclusions of up to 3  $\mu\text{m}$  were typically found in relatively small filaments with an average diameter of 4 - 5  $\mu\text{m}$  (Figure 10 A, C). They were evenly distributed in the filament with one big polyP granule per cell. A different pattern was present for smaller inclusions with around 0.5  $\mu\text{m}$  diameter, which were typically found in bigger filaments sized between 12 - 15  $\mu\text{m}$  (Figure 10 B, D). Here, several small polyP granules were unevenly distributed throughout the filaments and numbers of polyP granules differed between individual cells.

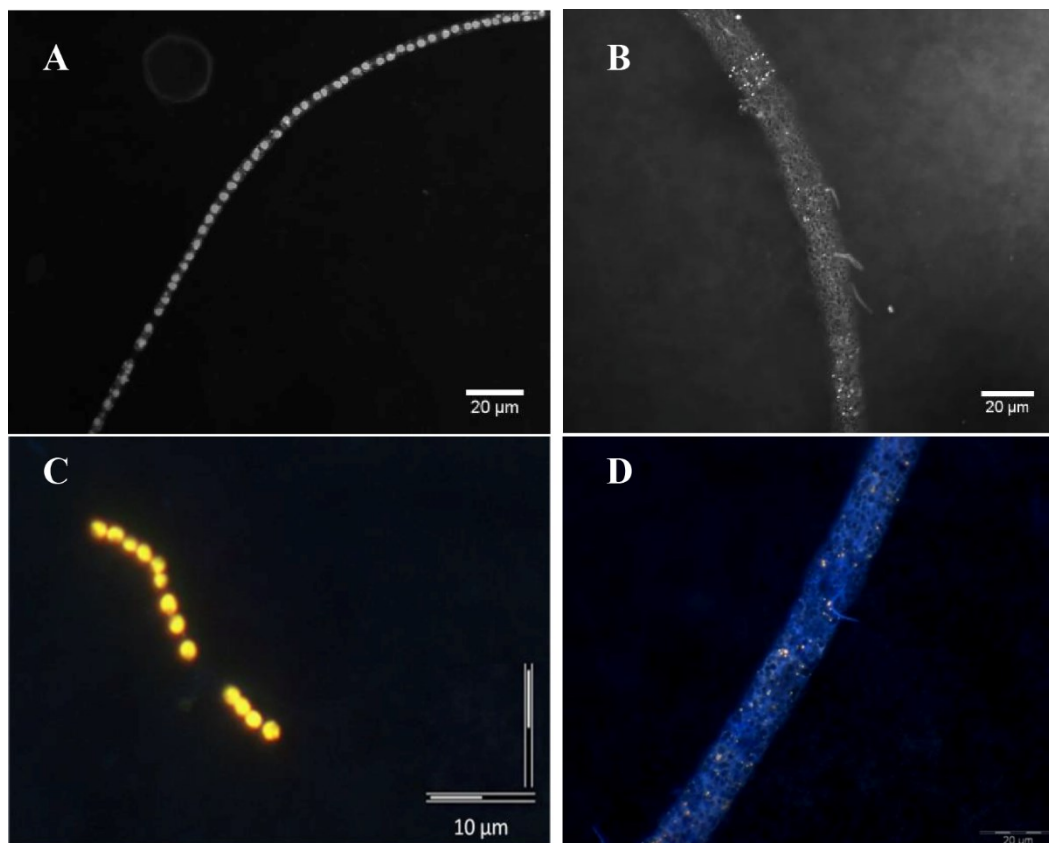


**Figure 10:** DAPI stained filaments of the family *Beggiatoaceae* with differently sized polyP inclusions. A + C: Big polyP inclusions in relatively small filaments with a diameter between 4 and 5  $\mu\text{m}$ ; B + D: Small polyP inclusions in relatively big filaments with diameters between 12 and 15  $\mu\text{m}$ .

### 3.2.2 Number, diameter distribution and biovolume of *Beggiatoa* filaments from the continental shelf off Peru

Analyzed *Beggiatoaceae* filaments were sampled from stations with 77 m, 200 m and 244 m total water depth to determine the abundance, the distribution of filament diameter and the biovolume of filaments present in these sediments. Filament numbers per  $\text{cm}^3$  showed minor differences between the three stations analyzed with means ranging from 316 filaments per  $\text{cm}^3$  sediment found at 200 m depth to 403 at 77 m depth and 455 at 244 m depth (Figure 11). The lowest mean with 316 filaments per  $\text{cm}^3$  at 200 m total depth was also accompanied with the highest standard deviation. .

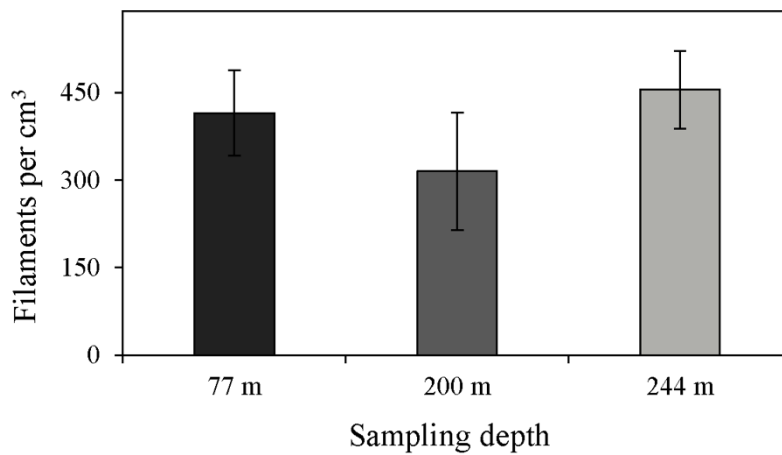


**Figure 11:** Means of filament counts from a minimum of five subsamples per cm<sup>3</sup> sediment at stations with maximum water depth of 77 m, 200 m and 244 m.

The filament diameter distribution of *Beggiatoaceae* filaments is shown in Figure 12. Diameters between 7.5 and 12  $\mu\text{m}$  were most abundant at the shallowest station at 77 m depth and represented 85% of all filaments. The smallest filaments found at this depth had a diameter of 5  $\mu\text{m}$ , whereas largest diameters reached up to 40  $\mu\text{m}$ . A dominance of thin filaments with diameters of only 2.5  $\mu\text{m}$  was present at the station with the highest water depth of 244 m. These filaments represented 44% of all filaments at this station followed by 20% filaments with a diameter of 3.8  $\mu\text{m}$  and 17% filaments with a diameter of 5  $\mu\text{m}$ . The biggest filaments found at this depth had diameters of 7.5 and 10  $\mu\text{m}$ , which constituted 10% and 8% of all filaments, respectively. A broad range of diameter distribution attributed to *Beggiatoa* filaments characterized the station with a maximum depth of 200 m. 30% of all filaments had a diameter of 3.8  $\mu\text{m}$ . Together with filaments with 10  $\mu\text{m}$  diameter (23% of all filaments) and filaments with a diameter of 12.5 (17%), these three size classes represented 70% of all filaments.



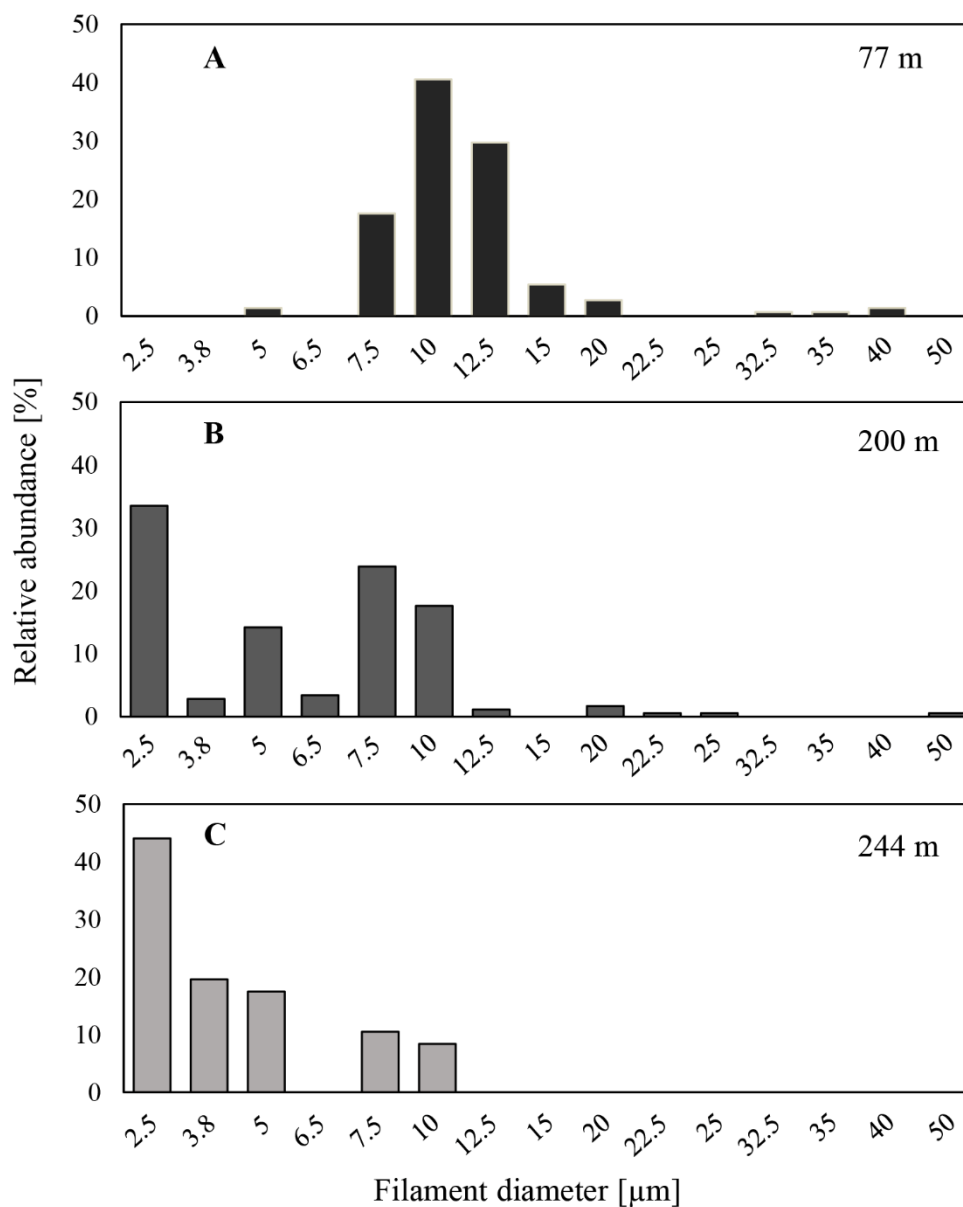


**Figure 12:** Relative abundances of filament diameter distribution of *Beggiatoa* across three sampled depth: 77 m (A); 200 m (B); 244 m (C).

The biovolume of *Beggiatoa* in sediments was determined by measuring length and widths of individual filaments (Material & Methods) and is presented in Figure 13. The biovolume of filaments per  $\text{cm}^3$  sediment was highest at 77 m depth with  $0.07 \text{ mm}^3$  filaments per  $\text{cm}^3$  sediment and sharply dropped to  $0.02$  and  $0.01 \text{ mm}^3$  filaments per  $\text{cm}^3$  sediment in 200 m and 244 m water depth.

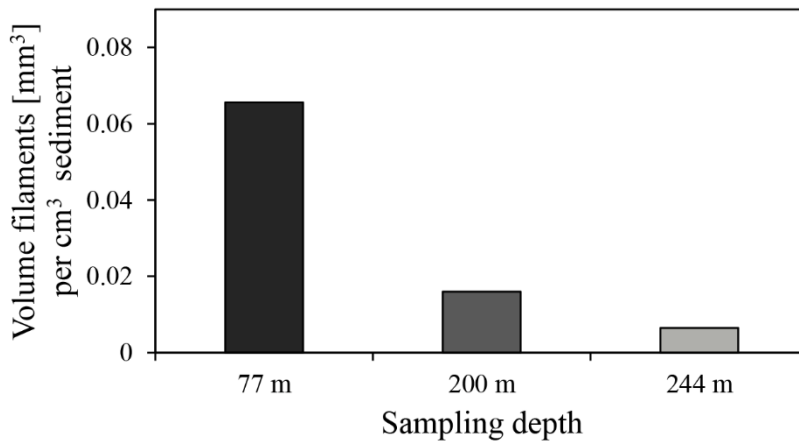


**Figure 13:** Biovolume of *Beggiatoaceae* filaments across three stations with water depths of 77 m (A), 200 m (B) and 244 m (C).

### 3.2.3 Quantitative analyses of polyP in *Beggiatoa*

For quantification of polyP in marine *Beggiatoa* spp., 100 filaments were picked in triplicates from three depths in the OMZ upwelling area in front of Peru: 77 m, 200 m and 244 m.  $P_i$ -equiv. in polyP per  $cm^3$  in three samples from 77 m and 244 m depth and two samples from 200 m depth are shown in Figure 14. Equivalentents per  $cm^3$  were lowest at 200 m depth with 5 – 6 nM. Higher concentrations were found at 77 m depth ranging between 8 – 10 nM. Highest variability between the three individual samples were present at 244 m depth, where concentrations of  $P_i$ -equiv. ranged between 6 and 15 nM in individual samples.

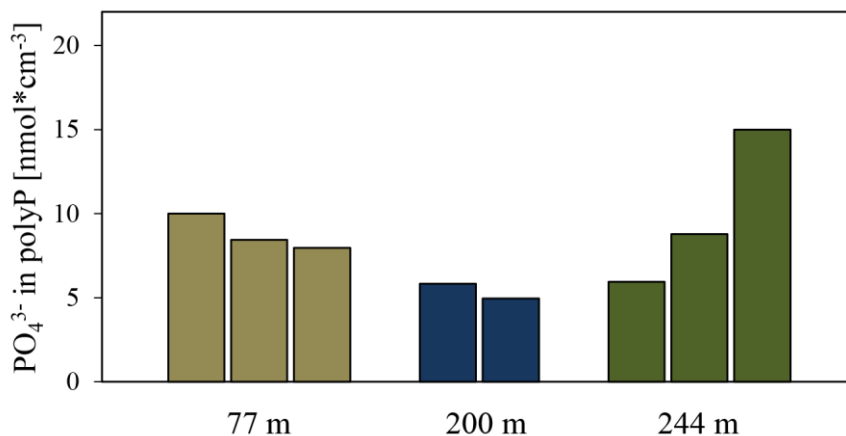


**Figure 14:** Concentrations of  $P_i$ -equiv. stored as polyP in *Beggiatoa* filaments present in one  $cm^3$  sediment.

### 3.3 NanoSIMS results

#### 3.3.1 Phosphorus and $^{18}\text{O}$ distribution in *Beggiatoa* sp. 35Flor after in situ incubations

NanoSIMS analyses revealed distinct distribution patterns of  $^{18}\text{O}$  enrichments and P counts throughout the filaments, which enabled the differentiation between ROIs assigned to polyP and ROIs assigned to cytoplasm (Figure 15).

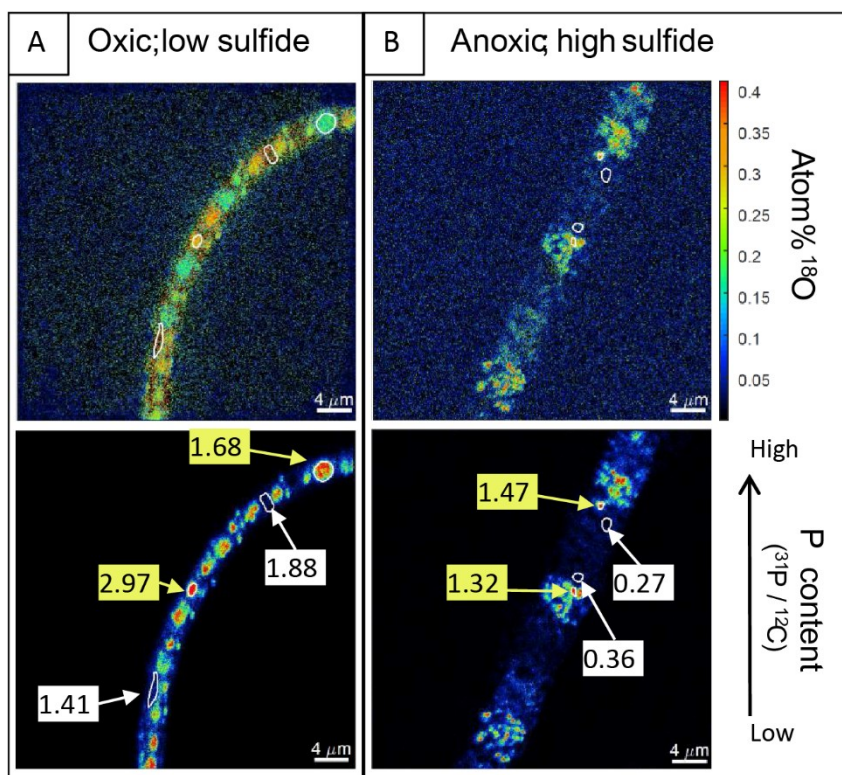


**Figure 15:** “The distributions of  $^{18}\text{O}$  and P are shown for the physiological most distinguishable incubation conditions. (A) Optimal growth condition (oxic, low sulfide); (B) stressful condition (anoxic, high sulfide flux).  $^{18}\text{O}$  enrichments in atom% are presented in the top panels, and phosphorus content normalized to carbon is presented in the bottom panels with two exemplary ROIs for both polyP (yellow regions) and cytoplasm (white regions), defined by manual assignment” (Langer et al., 2018)

Relative P content (C/P) plotted against  $^{18}\text{O}$  enrichments revealed the threshold value of 18 for C/P to differentiate between polyP and cytoplasm (Figure 16, Langer et al., 2018).

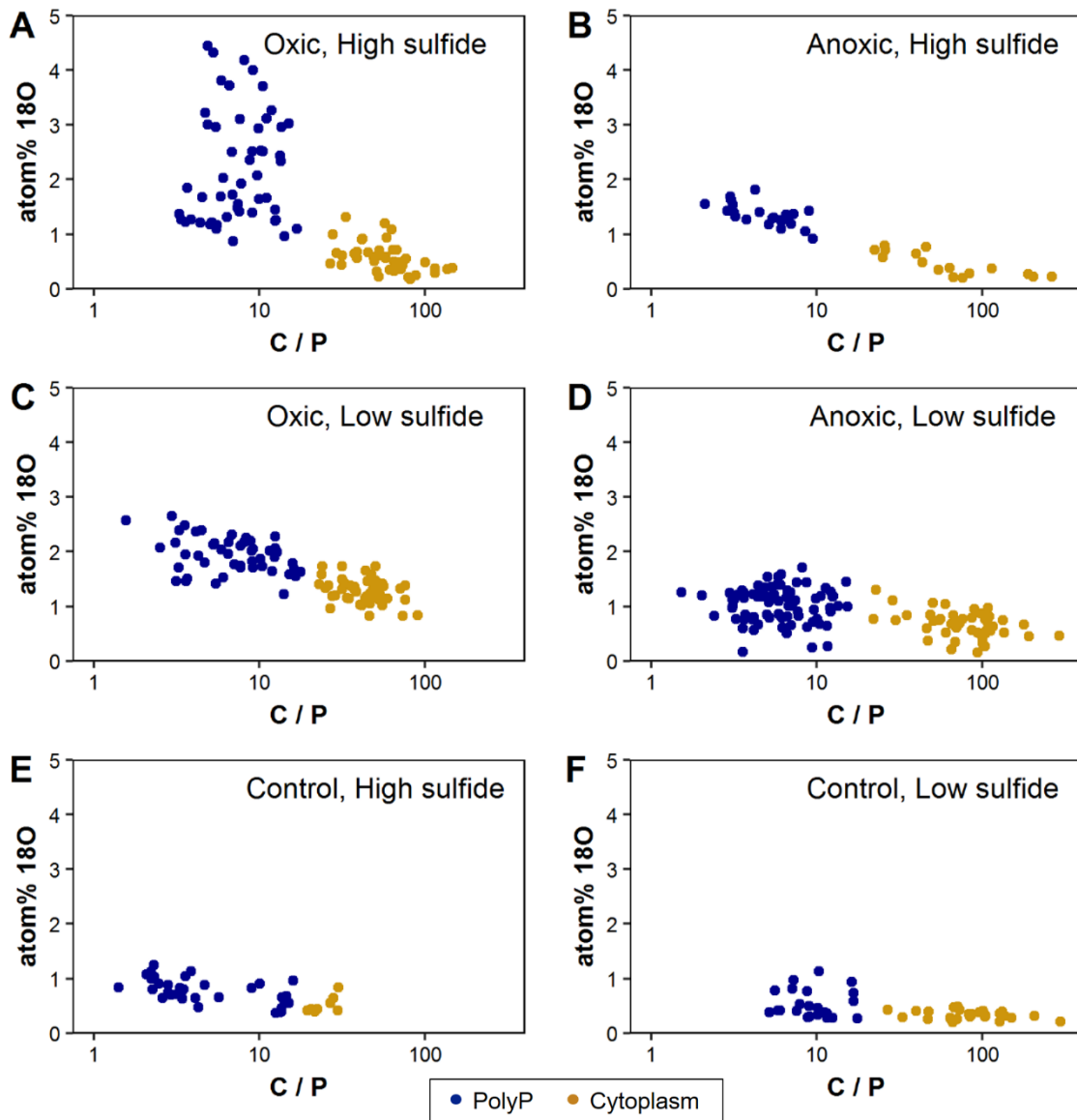


**Figure 16:** “C/P ratios, indicative of P content, plotted against  $^{18}\text{O}$  enrichments for all determined ROIs. Decreased C/P ratios (high P content) are apparent in areas defined as polyP compared to regions defined as cytoplasm, especially under high sulfide condition” (Langer et al., 2018).

Elemental distributions of  $^{31}\text{P}$  and  $^{18}\text{O}$  in *Beggiatoa* are shown in Figure 17 and Figure 18. Filaments were exposed to low (Figure 17) and high (Figure 18) sulfide concentrations during “oxic” (17 A), “anoxic” (17 B) and “control” (17 C) treatments (see Material and Methods). The presence of distinct P rich areas became apparent in filaments after all incubation conditions and signal intensity did not differ between treatments exposed to low or high sulfide fluxes (in contrast to sulfur counts, see below). Large spherical P inclusions accompanied with some smaller granules were present in every single cell of filaments exposed to low sulfide fluxes and incubated under continuous micro-aerobic conditions (oxic

incubation, Figure 17 A). The distribution of P in filaments grown under identical low sulfide fluxes, but incubated with  $\text{H}_2^{18}\text{O}$  during anoxic conditions, revealed several small P inclusions, which were uniformly distributed throughout the filament.

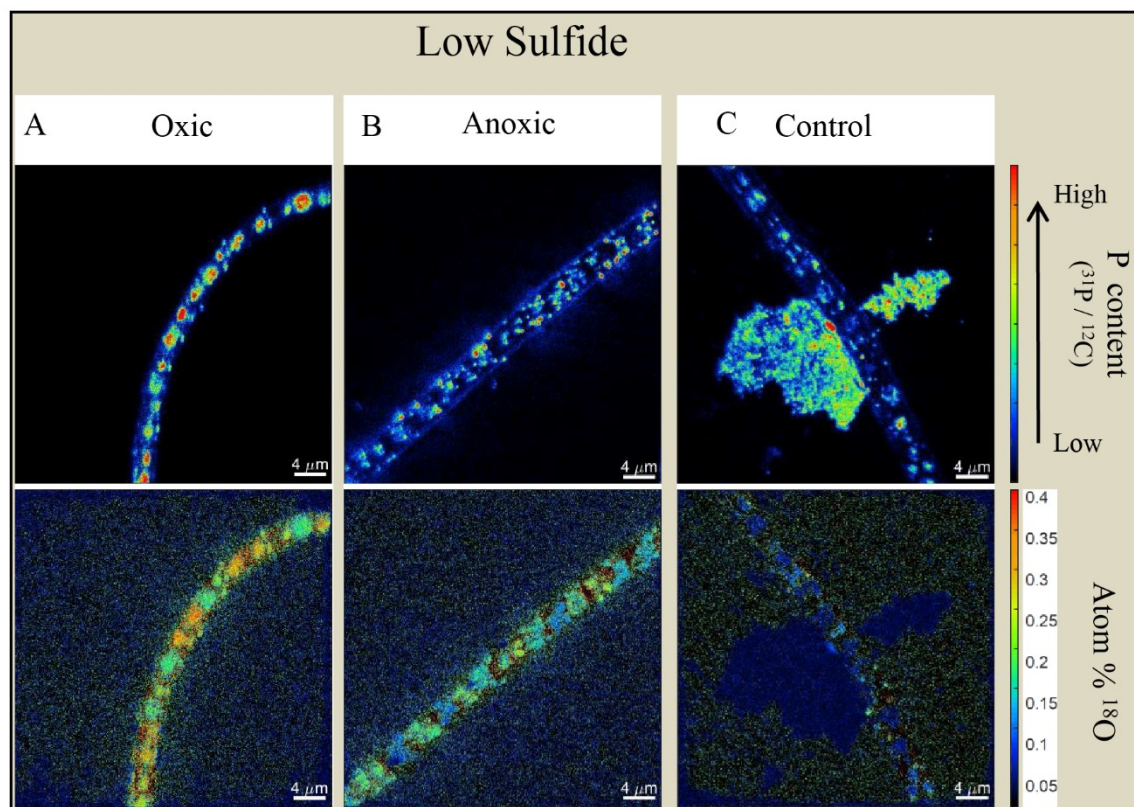


**Figure 17:** P (upper panel) and  $^{18}\text{O}$  (lower panel) distribution in filaments which were exposed to low sulfide fluxes and incubated under oxic (A), anoxic (B), and cooled (= control, C) conditions.

P signals appeared to be less regularly distributed between cells of filaments when incubated under high sulfide fluxes (Figure 18). In contrast, “aggregated” P signals appeared to be present only in some cells of the filaments with barely any P signals in neighboring cells. This was especially pronounced during anoxic incubation conditions (Figure 18 B), but was also found after oxic incubation (Figure 18 A). P signals in filaments incubated at 4 °C (control, Figure 18 C) were generally weak and partly masked by some agar impurities on the filter, which interfered with the nanoSIMS measurements.

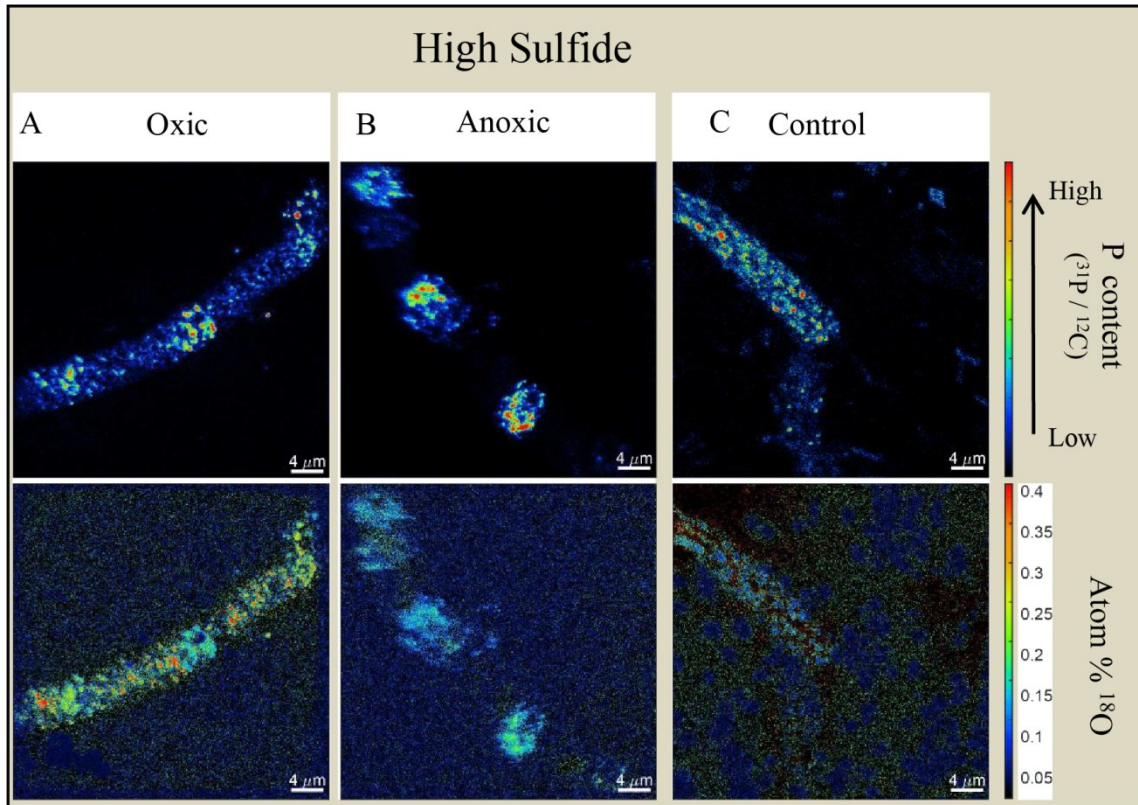


**Figure 18:** P (upper panel) and  $^{18}\text{O}$  (lower panel) distribution in filaments which were exposed to high sulfide fluxes and incubated under oxic (A), anoxic (B), and cooled (= control, C) conditions.

$^{18}\text{O}$  enrichments were above the natural background of 0.2 atom% in most treatments based on visual inspection (Figure 17, Figure 18 lower panel), with varying intensities and distribution patterns between high and low sulfide treatments. Enrichments in high sulfide treatments seemed to be restricted to P rich spots, associated with low enrichments in neighboring regions with less intense P signals (Figure 18). In contrast,  $^{18}\text{O}$  enrichments in low sulfide treatments were distributed over the whole filament and not restricted to P signals after both oxic and anoxic incubation conditions (Figure 17). Clearly, less intense  $^{18}\text{O}$  enrichments were present in filaments incubated at 4 °C, irrespective of the sulfide fluxes.

### 3.3.2 Differences between defined regions of interest (ROIs)

Figure 19 shows boxplots with  $^{18}\text{O}$  enrichments in ROIs, defined to differentiate between polyP and cytoplasm (see Materials and Methods) for all treatments (oxic, anoxic, control) incubated under low (A) and high (B) sulfide fluxes.

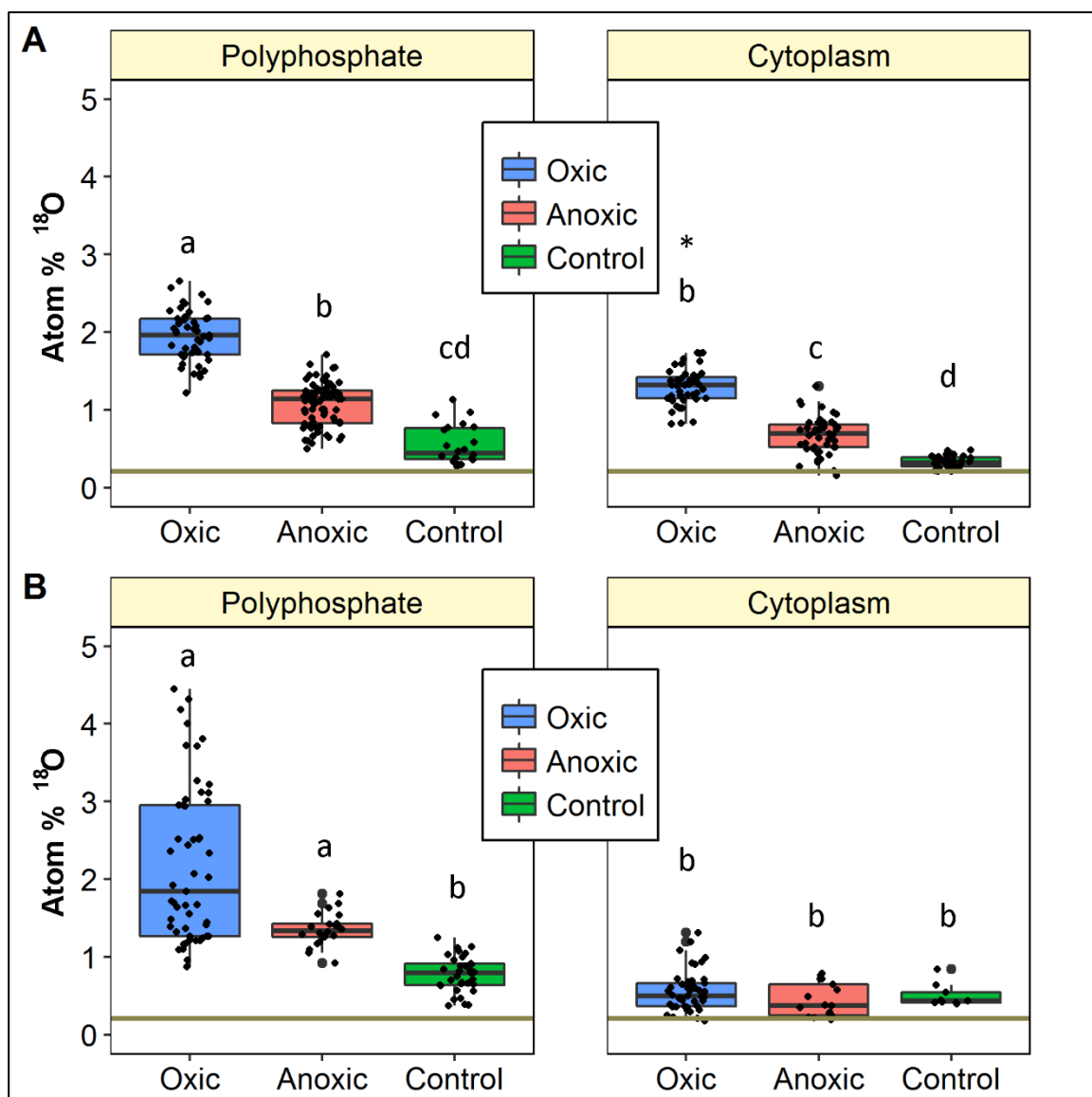


**Figure 19:** “Boxplots from ROIs based on P counts for different treatments (oxic, anoxic, control) during low sulfide flux (A) and high sulfide flux (B). Different letters indicate boxes that differ significantly between treatments exposed to the same sulfide fluxes ( $P < 0.05$ ). Boxes with same letters are not significantly different ( $P > 0.05$ ). The asterisk indicates the box being significantly different between different sulfide concentrations within the same treatment. The horizontal line at 0.2 atom% presents the natural abundance of  $^{18}\text{O}$ ” (Langer et al., 2018).

No significant different  $^{18}\text{O}$  enrichments in polyP and the cytoplasm were found between low and high sulfide concentrations for anoxic and control treatments. The only significant difference between high and low sulfide fluxes within the same treatment was present after oxic incubation in ROIs defined as cytoplasm.

ROIs defined as polyP in the low sulfide oxic incubation were significantly higher enriched than polyP and the cytoplasm after anoxic and cooled control incubations with maximum

enrichments of 2.7 atom%  $^{18}\text{O}$  (Figure 19, Table 2). Enrichments in polyP in the low sulfide anoxic treatment were significantly higher than enrichments in ROIs defined as cytoplasm in the same treatment (anoxic, low sulfide) and also higher compared to enrichments in polyP and the cytoplasm of the control treatment (control, low sulfide). No significant different enrichments were present between ROIs defined as polyP in the anoxic treatment and ROIs defined as cytoplasm in the oxic treatment.  $^{18}\text{O}$  enrichments were similar between polyP and cytoplasm areas in the control treatment. Enrichments in the control incubation were significantly lower than in the oxic and anoxic treatments for both ROIs defined as polyP and cytoplasm. Enrichments in the control incubation were up to 0.5 atom%  $^{18}\text{O}$  in ROIs defined as cytoplasm, and up to 1.1. atom%  $^{18}\text{O}$  in ROIs defined as PolyP (Table 2, Table 3).

**Table 2:** Minimum and maximum  $^{18}\text{O}$  enrichments [atom%] for ROIs defined as polyP.

	PolyP			
	Low sulfide		High sulfide	
	Minimum	Maximum	Minimum	Maximum
Oxic	1.2	2.7	0.9	4.5
Anoxic	0.5	1.7	0.9	1.8
Control	0.3	1.1	0.4	1.3

Barplots with  $^{18}\text{O}$  enrichments in ROIs from filaments exposed to high sulfide fluxes are shown in Figure 19 B. Enrichments in ROIs defined as polyP in the oxic treatment showed high variability and contained the highest  $^{18}\text{O}$  enrichments of all incubations with up to 4.5 atom% (

Table 3). ROIs defined as polyP in oxic and anoxic treatments were significantly higher enriched than all ROIs defined as cytoplasm in all other treatments. ROIs in the cytoplasm were comparatively low enriched and showed no significant differences between the treatments (oxic, anoxic, control). Enrichments in ROIs defined as polyP in the control were significantly lower compared to enrichments in polyP after oxic and anoxic treatment, but did not differ significantly in the cytoplasm between all treatments.



**Table 3:** Minimum and maximum  $^{18}\text{O}$  enrichments [atom%] for ROIs defined as cytoplasm.

	Cytoplasm			
	Low sulfide		High sulfide	
	Minimum	Maximum	Minimum	Maximum
Oxic	0.8	1.7	0.2	1.3
Anoxic	0.2	1.3	0.2	0.7
Control	0.2	0.5	0.4	0.8

Ratios between mean enrichments of  $^{18}\text{O}$  in ROIs defined as polyP and defined as cytoplasm are shown in Table 4. Highest ratios were present in high sulfide treatments after both oxic (ratio: 3.9) and anoxic (ratio: 3.0) incubations. Comparable ratios between 1.4 and 1.6 atom%  $^{18}\text{O}$  were found after low sulfide oxic incubation and both control incubations.

**Table 4:** “Mean values of  $^{18}\text{O}$  enrichments in ROIs defined as polyP and as cytoplasm and the ratio between the means of enrichments in polyP and cytoplasm. It becomes evident that the ratio is distinctively higher in treatments exposed to high sulfide fluxes, both under oxic and under anoxic conditions” (Langer et al., 2018).

	Mean $^{18}\text{O}$ enrichments [atom%]					
	Oxic High $\text{H}_2\text{S}$	Oxic Low $\text{H}_2\text{S}$	Anoxic; High $\text{H}_2\text{S}$	Anoxic; Low $\text{H}_2\text{S}$	Control; High $\text{H}_2\text{S}$	Control; Low $\text{H}_2\text{S}$
ROIs PolyP	2.2 SD = 1.0 n = 53	2.0 SD = 0.3 n = 48	1.4 SD = 0.2 n = 22	1.1 SD = 0.3 n = 78	0.8 SD = 0.2 n = 36	0.5 SD = 0.2 n = 23
ROIs Cytoplasm	0.6 SD = 0.2 n = 44	1.3 SD = 0.2 n = 44	0.4 SD = 0.2 n = 17	0.7 SD = 0.2 n = 45	0.5 SD = 0.2 n = 10	0.3 SD = 0.1 n = 29
<b>PolyP / Cytoplasm</b>	<b>3.9</b>	<b>1.5</b>	<b>3.0</b>	<b>1.6</b>	<b>1.6</b>	<b>1.4</b>

### 3.3.3 Sulfur distribution in *Beggiatoa* sp. filaments after in situ incubations

Sulfur signals in filaments grown with low sulfide fluxes are shown in Figure 20. Distribution and intensity of sulfur counts obtained from nanoSIMS were similar between oxic, anoxic

and control treatments. Ratios of S normalized to  $^{12}\text{C}^{14}\text{N}$  also showed only minor differences between the treatments. Intensity and amount of S counts were distinctly higher in filaments grown with high sulfide fluxes after control and oxic treatments than in all treatments exposed to low sulfide fluxes (Figure 20). In addition, a much higher density of sulfur globules was present in these two treatments compared to treatments grown with low sulfide fluxes, which was especially pronounced in the oxic treatment. A much lower S content was present in filaments incubated under anoxic conditions (Figure 21 C). Signal intensities of sulfur were much less pronounced accompanied by decreased numbers of sulfur globules. S signals in the control treatment were similar to counts in the oxic treatment.

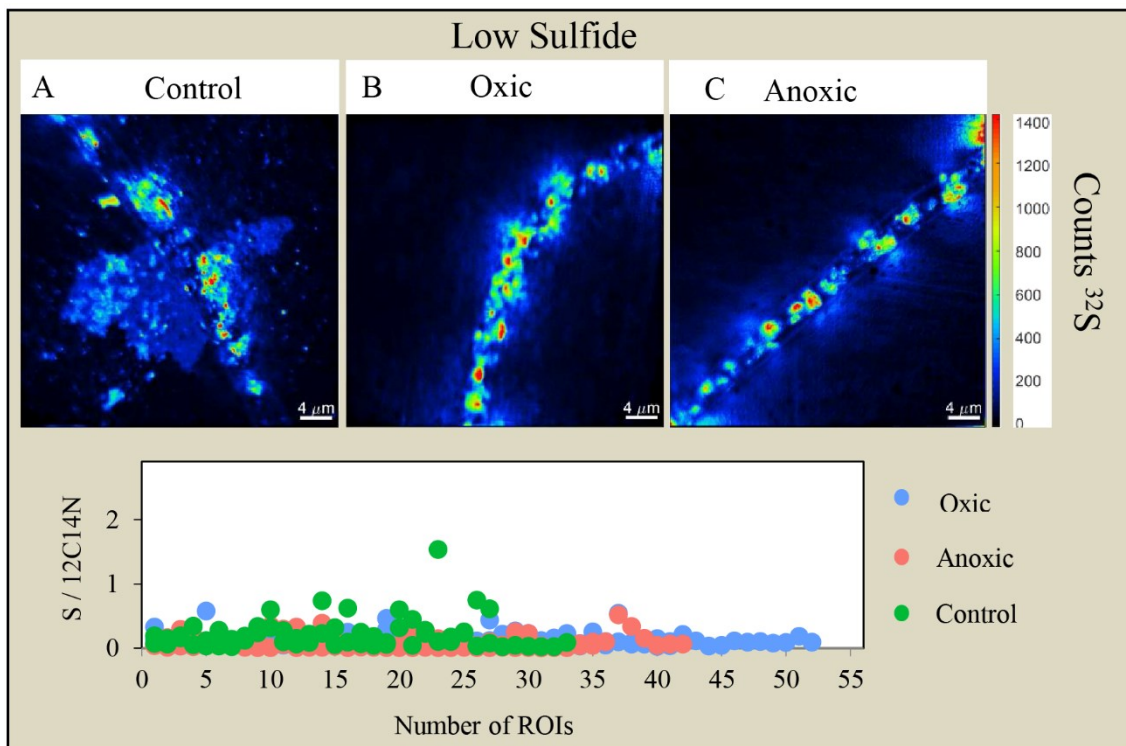


**Figure 20:** Sulfur counts in low sulfide treatments for Control (A), Oxic (B) and Anoxic (C) incubations.

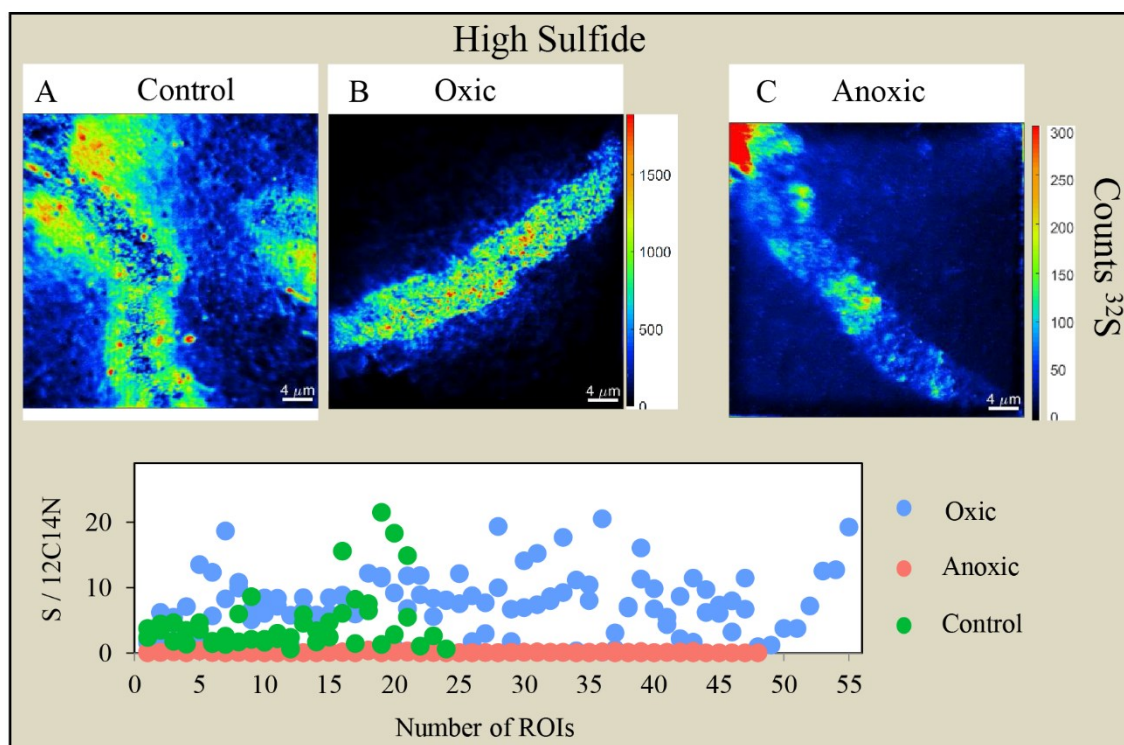


**Figure 21:** Sulfur counts in high sulfide treatments for Control (A), Oxic (B) and Anoxic (C) incubations.

### 3.3.4 Ex situ incubations of sediment cores from the Peruvian upwelling

Visual discernible P content and  $^{18}\text{O}$  enrichments in relatively P rich and relatively P poor ROIs in filaments incubated under ex situ conditions are presented in Figure 22. P content presented as P/C ratios was similar in all four filaments shown.  $^{18}\text{O}$  enrichments in ROIs defined as polyP were significantly higher than ROIs defined as cytoplasm in filaments A and B. No significant difference between polyP and cytoplasm was present in filaments C and D.

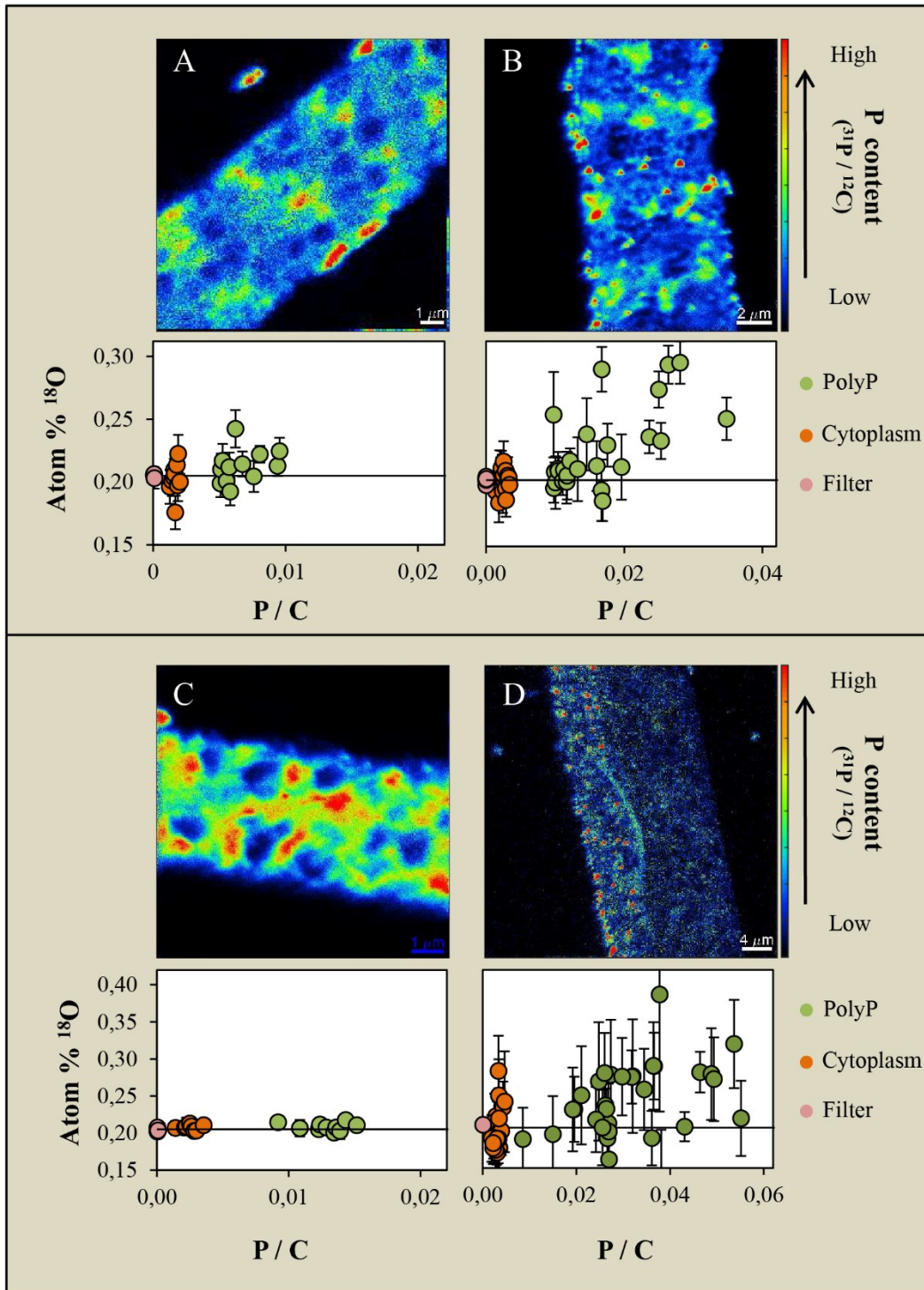


**Figure 22:** Upper panels: nanoSIMS counts of P signals in four different filaments after 24 h ex situ incubation with  $^{18}\text{O}$ -water. Lower panels:  $^{18}\text{O}$  enrichments in P rich spots (green) and P poor spots (orange).  $^{18}\text{O}$  enrichments in ROIs defined as polyP were significantly higher than ROIs defined as Cytoplasm in filaments A + B.

## 4 Discussion

### 4.1 Quantities and relevance of polyP in coastal and marine environments

#### 4.1.1 PolyP in a coastal area of the Baltic Sea

PolyP quantification with DAPI was based on polyP standards with polyP chain lengths consisting of 45  $P_i$  residues (see Material and Methods). The following discussion will always refer to polyP being synonymous with  $P_i$  equiv. in polyP. This expresses the number of  $P_i$  residues being present in quantified polyP found in environmental samples.

PolyP concentrations showed high spatial and temporal variations in bottom water samples of coastal waters in front of the nature reserve Heiligensee and Hütelmoor. High spatial differences are evident when comparing concentrations at station 1, located close to the shore and station 3 being more offshore but with only several 100 m distance. Despite the close spatial proximity, polyP concentrations varied considerably in June. Also at stations 35 and 15 strong variations are discernible with distinctly higher polyP concentrations at station 15 in July and December, compared to concentrations at station 35 during the same months. This is especially pronounced in samples from July where the overall highest concentration was present at station 15 and the overall lowest concentration at station 35 during the same sampling month July in 2016. Consequently concentrations were highly variable and did not show any regional trend between stations being in direct proximity to the coast and stations being slightly more offshore.

Intracellular polyP formation depends on environmental redox conditions and is thought to generally occur via luxury uptake mechanisms (details in 4.2). This requires sufficiently high  $P_i$  concentrations in the surrounding environment being expected to occur at coastal stations. Near shore environments are characterized by high loads of organic matter, which can be the consequence of high rates of primary production, riverine input or submarine groundwater discharge (SGD) (Kotwicki et al., 2014; Ask et al., 2016). As a consequence, organic matter remineralization is increased with concurrent release of inorganic nutrients like  $P_i$ , potentially supporting formation of polyP. However, stations with close proximity to the coast did not show consistently higher polyP concentrations than present at stations more offshore. This could be explained by the medium to coarse permeable sands prevailing in the first meter in sediments of the study site (Kreuzburg et al., 2018), which are characterized by generally lower organic carbon contents (e.g. Hüttel & Rusch, 2000). Therefore, input of reactive carbon in these sediments primarily depend on groundwater inputs or circulating seawater

driven by advective transport processes. The latter is more dominant in sandy sediments than in muddy sediment (Janssen et al., 2005) and would lead to comparable concentrations of nutrients in bottom water and pore water. This is confirmed in pore water samples from three stations (Figure 7 A) showing similar concentrations of polyP as generally present in bottom water samples. This could be enabled through a potentially regular flushing of the permeable sediments through advection. The suspected high permeability of these sandy sediments might explain the uniform polyP concentrations found in these pore waters and the overlaying bottom waters. In contrast, distinctly higher polyP concentrations were found in pore waters from the other three stations in 30 – 50 cm depth (Figure 7 B). This indicates substantial environmental differences prevailing at these sites, especially at station D with more than 1.5  $\mu\text{M}$  polyP. This could be due to a high abundance of polyP accumulating bacteria through favorable polyP formation conditions, which could be reasoned by locally present submerged peats (Kreuzburg et al., 2018). These organic rich deposits could potentially be responsible for an elevated release of nutrients to overlain waters (Kieckbusch & Schrautzer, 2006) and would prevent a deep mixing with water by advection caused by very low permeability of peat deposits (Rezanezhad et al., 2016).

As mentioned before, coastal zones can be impacted by SDG being another contributor to locally different nutrient regimes in bottom and pore water, which is supposed to occur in the study area (Juransinski & Janssen et al., 2018). SGD input fluxes on a global scale have been estimated to be comparable to water masses entering the ocean via rivers (Kwon et al., 2014, Cho & Kim, 2016) and could have, therefore, large implications on biogeochemical cycles. Since fluxes of dissolved inorganic P and dissolved inorganic N could be 50% higher than those entering coastal seas via rivers (Cho et al., 2018), SGD could support phytoplankton blooms or formation of intracellular polyP through elevated  $P_i$  concentrations in the water column. The expected local hotspots could be one factor explaining spatial differences in polyP concentrations patterns. SGD water masses may directly come from groundwater originating from the Hütelmoor being rich in nutrients, or from recycled Baltic Sea water which got enriched in nutrients when pushed through the seabed. Samples from groundwater in the Hütelmoor had considerably higher polyP content than present in bottom waters (Figure 8) being also accompanied by higher  $P_i$  concentrations than found in bottom waters of the Baltic Sea (M.Ibenthal, person. communication). This indicates the possibility for a luxury uptake mechanism comparable to waste water treatment plants, where varying oxygen concentrations lead to an uptake or release of  $P_i$  (McMahon & Read, 2013). Similar varying

oxygen regimes can be assumed for these groundwaters. The mixing of seawater and groundwater with different oxygen concentrations is often accompanied with the formation of redoxclines (Santoro, 2010), which in particular affects polyP metabolism. Since the groundwater wells are located close to the dune they are regularly flushed with seawater (M.Ibenthal, pers. communication). This leads to a regular supply with oxygen supporting polyP formation, followed by stagnation periods leading to oxygen depleted groundwaters and polyP degradation. Coastal zones are also influenced by mixing processes occurring in shallow waters, which lead to a uniform distribution of dissolved substances with no punctual input source present. Rivers generally have high P concentrations from agricultural inputs, which are transported to the sea and, therefore, connect the P sources from land with the Sea (Ruttenberg 2014). The study area in front of the Hütelmoor is influenced by the Warnow river estuary being ca 10 km west from the study area. Water masses entering the Baltic Sea are subjected to Coriolis forcing and deflected to the right being supported by mainly westerly winds (Jurasinski & Janssen et al., 2018). The increased nutrient loads being present in rivers like the Warnow (Freese et al., 2007) do likely influence the study area and also lead to higher  $P_i$  concentration which would influence polyP metabolism.

The difficulties in trying to conclude trends concerning spatial distribution patterns is also apparent when trying to assess seasonal variations. Samples originated from spring (April), summer (June, July), autumn (September, October) and winter (December). Concentrations of polyP varied between the samples, but did not show any solid trend. This is exemplarily reflected in samples obtained at station 11 and 15, where concentrations did only differ marginally between spring, summer, and winter (Figure 6). Since polyP metabolism is suspected to be substantially influenced by ambient  $P_i$  concentrations, one could assume to find differences in polyP concentrations depending on current statuses of bacteria- and phytoplankton blooms, which lead to a depletion of nutrients (Bunse et al., 2016). The increased presence of phytoplankton during favorable bloom conditions could lead to higher polyP values being quantified with the DAPI method, since filtering of the bulk water mass includes both bacteria- and phytoplankton. Despite the difficulties in concluding on spatial or seasonal tendencies in polyP concentration patterns, the continuous presence of polyP argues for a non-negligible potential P source. Ambient  $P_i$  concentrations in bottom waters ranged from 0.1 – 0.3  $\mu\text{M}$  (J. Westphal, person. communication) indicating non limiting P conditions during time of sampling. This points in principle to conditions enabling luxury uptake of  $P_i$  to synthesize polyP. Considering a polyP pool consisting of up to 0.12  $\mu\text{M}$   $P_i$

residues, stored polyP has the potential to substantially contribute to the local P cycling. However, this seems to be unlikely to occur since an intensive degradation with subsequent  $P_i$  release is normally assumed to occur during anoxic conditions and not in the well mixed oxic water column. Rather it indicates that the quantified background polyP concentrations of phyto-/ and bacterioplankton are indispensable for standard metabolic processes like ATP synthesis and are, therefore, not involved in potential polyP degradation with associated  $P_i$  release.

### 4.1.2 PolyP in the pelagic zone off Peru

Concentrations of polyP were relatively constant at station with 128 m maximum depth (Figure 9 A) with around 10 nM  $P_i$ -equiv. This is considerably lower than results obtained from a coastal zone of the Baltic Sea (4.1), but similar to results obtained from measurements at station ALOHA north of Hawaii. Here, polyP concentrations were highest in spring with around 8 nM in the first 50 m of the water column, representing about 10% of the total particulate phosphorus pool (Diaz et al., 2016). Concentrations were slightly lower in fall, but decreased in both seasons down to 2 nM at 15 water depth (Diaz et al., 2016). In contrast to the station with a maximum water depth of 128 m, polyP concentrations showed a slight decrease at the station with 244 m maximum water depth (Figure 9 B). PolyP was twice as high compared to the remaining samples before it decreased to 10 nM. A retention of polyP in surface waters was demonstrated in the oligotrophic Sargasso Sea and was assumed to be released from sinking particles under environmental stress (Martin et al., 2014). This also underlines that polyP metabolism is not restricted to  $P_i$  rich environments. However, similar mechanisms as present in the Sargasso Sea are unlikely to occur in the surface waters off Peru, because a steady supply with nutrient rich upwelling waters prevails (Ehlert et al., 2015; Steinfeldt et al., 2015). Instead, polyP cycling is more relevant in the sediments as shown in the following.



## 4.2 Contribution of biologically stored polyP to sedimentary P fluxes

### 4.2.1 Filamentous Sulfur bacteria in Peruvian upwelling areas

Filamentous sulfur bacteria have been regularly found in sediments off the south-west American coast, predominantly in front of Chile and Peru (Gallardo 1977, Mosch et al., 2012., Sommer et al., 2016). They have been observed to form dense white mats, which varied in densities between different seasons due to oscillating redox conditions controlled by the frequency and strength of oxygenation events (Gutiérrez et al., 2008). Studies about filamentous sulfur bacteria in the Peruvian/Chilean upwelling area have been primarily focused on *Marithioploca* (e.g. Schulz et al., 1996, 2000; Levin et al., 2002, Holmkvist et al., 2010) in contrast to only few studies focusing on the abundance of *Beggiatoa*. Instead, conclusions about the presence of *Beggiatoa* were inferred from visual analyses (Mosch et al., 2012, Sommer et al., 2016) which cannot discriminate between *Beggiatoa* and *Marithioploca*. Biovolumes of *Beggiatoa* filaments were found to be around  $5 \text{ mm}^3 \cdot \text{cm}^{-3}$  in the Peruvian upwelling zone in 256 m water depth sampled during a cruise in 2005 (Arning et al., 2008). Biovolumes of *Beggiatoa* analyzed in this study were comparably low with only  $0.06 \text{ mm}^3 \cdot \text{cm}^{-3}$  at 77 m depth to less than  $0.01 \text{ mm}^3 \cdot \text{cm}^{-3}$  at 244 m depth. Since the presence of *Beggiatoa* is highly dependent on the prevailing redox conditions, it is likely that the dominating low oxygen conditions during the sampling period in May 2017 restricted growth of *Beggiatoa* to similar high densities (Table 6). Especially the oxygen depleted bottom waters at 244 m water depth did not support dense bacterial mats formed by *Beggiatoa* filaments.

**Table 5:** In situ bottom water oxygen concentrations during sediment sampling (Data: Clemens et al., unpublished)

Depth	Oxygen concentration [ $\mu\text{M}$ ]
77 m	5.7
129 m	1.6
244 m	0

Despite the diverging biovolumes of *Beggiatoa* at the three analyzed depths, the filament numbers varied only marginal with depth (Figure 11). Filament numbers were comparable to abundances of *Beggiatoa* found in arctic sediments, which also varied in their biovolume

despite of similar filament numbers between different stations (Jørgensen et al., 2010). The huge differences between biovolumes with concurrent stable filament numbers between 77 – 244 m are reasoned in the varying distribution of filament diameters (Figure 12). The varying dominance of different filament diameter indicates different species distribution patterns. For example, the filament diameter of the well-studied strain *Beggiatoa* sp. 35Flor is around 6  $\mu\text{m}$  (Kamp et al., 2008) compared to 30  $\mu\text{m}$  and 60  $\mu\text{m}$  diameters present in *Candidatus* *Isobeggiatoa* sp. and *Candidatus* *Maribeggiatoa* sp., respectively (McKay et al., 2012, Jean et al., 2015). However, deducing phylogenetic relations based on morphological criteria is usually misleading and should reliably be determined by phylogenetic analyses (Salman et al., 2011).

### 4.2.2 Presence and size of polyP inclusion in filamentous sulfur bacteria

Members of the family *Beggiatoaceae* were reported to have the capability of storing extraordinary high amounts of polyP (e.g. Schulz & Schulz, 2005, Brock et al., 2012). This trait was also linked to the genus *Marithioploca*, which is present in sediments of the Peruvian upwelling system, reasoned in a correlation of *Marithioploca* 16SrRNA genes with sedimentary  $\text{P}_i$  release (Lomnitz et al., 2016). However, earlier laboratory studies did not find hints on excessive polyP storage by *Marithioploca* after activity assays with microradioautography (MAR) and  $^{33}\text{P}$  (Hogslund et al., 2009), which was also supported by fluorescent microscopy aimed to identify polyP conducted in scope of this thesis. Therefore, *Marithioploca* were not considered for detailed analyses (Section 3. Results). However, fluorescent microscopy revealed the presence of polyP inclusions with up to 3  $\mu\text{m}$  (Figure 10 A + C) in diameter found in filaments attributed to *Beggiatoa*. These large inclusions are among the biggest bacterial polyP inclusions found in environmental samples. Size and form are similar to inclusions being reported from the cultured strain *Beggiatoa* sp. 35Flor (Brock et al., 2012). The presence of these large sized polyP inclusion in the field is particular remarkable, since hitherto polyP inclusions reported from field samples of filaments in the *Beggiatoaceae* family have typically not exceeded diameters of 2  $\mu\text{m}$ . This was shown for example in *Beggiatoa* spp. analyzed from hypersaline coastal lagoons in Brasil (de Albuquerque et al., 2010) or in the marine genus *Thiomargarita* sp. (Schulz & Schulz, 2005). *Beggiatoa* spp. from the Peruvian sediments with larger diameters were found to have several smaller polyP inclusions (Figure 10 B + D), which sizes resemble those found in the type

strain *Beggiatoa alba* (Salman et al., 2011, Havelmeyer, 2013). The P content in polyP was demonstrated to be exponentially dependent on polyP diameter making big bacteria much more relevant when analyzing microbially stored polyP, even when occurring in lower number than small bacteria (Schulz-Vogt et al., 2019). This underlines the potential contribution of the *Beggiatoa* species with big polyP inclusions to contribute to the observed sedimentary  $P_i$  fluxes, particularly in 200 m and 244 m depth where the smaller sized *Beggiatoa* filaments with large polyP inclusions dominated (Figure 12). On the other hand, bigger sized *Beggiatoa* species with smaller polyP inclusions contained not only one polyP granules as typically present in non- filamentous bacteria like *Sulfurimonas* sp. (Möller et al., 2018), but contained several small inclusions distributed over the whole filament (Figure 10 B + D ). This opens the possibility for an equal contribution to sedimentary  $P_i$  fluxes from *Beggiatoa* from different size classes and differently sized polyP inclusions, also at 77 m depth, where the diameter sizes with several small polyP inclusions dominated. In general, the presence of different sized polyP inclusion in different *Beggiatoa* species within the same environmental area indicates different prevailing polyP accumulating mechanisms between different species within the genus *Beggiatoa*.

#### 4.2.3 Contribution of PolyP storage to sedimentary phosphate release

Sedimentary polyP has been shown to be abundant in OMZs (Kraal et al., 2015) and elevated  $P_i$  release rates were repeatedly reported for sediments off Peru (Noffke et al., 2012, Lomnitz et al., 2016). The polyP inclusions found by fluorescent microscopy in large filamentous sulfur bacteria supports the possibility for a biologically mediated contribution to sedimentary  $P_i$  release. This was suggested for *Beggiatoa* (Noffke et al., 2012) and *Marthioplaca* (Lomnitz et al., 2016) even though laboratory experiments did not show polyP formation by the latter organisms (Hogslund et al., 2009). A contribution of *Beggiatoa* or other large sulfur bacteria has been considered as a relevant, hitherto overlooked contributor to sedimentary  $P_i$  release, since up to 50% of the measured  $P_i$  fluxes were not explained at the Peruvian Shelf by a recently conducted P mass balance based on geochemical parameters (Lomnitz et al., 2016).  $P_i$  equivalents in polyP stored by *Beggiatoa* measured in this study substantially differed in the three samples from 244 m depth from which one sample contained highest concentrations found compared to all other samples (Figure 14). Filaments with small sized diameters and large polyP inclusions dominated at this depth, which would

support the linkage between large sized polyP inclusions with high P content as demonstrated in the Black Sea with the presence of large polyP granules in magnetotactic bacteria (Schulz-Vogt et al., 2019). However, the remaining two samples contained considerably lower  $P_i$ -equiv. in polyP which were similar to quantities found in filaments from 77 m and 200 m dept. Instead, the polyP content across the three sampled depths showed no significant differences despite the alternating filament diameter distributions with different types of polyP inclusions (Figure 10, Figure 12) and different bottom water oxygen concentrations (Table 5). Therefore, the presence of differently sized polyP inclusions has no significant impact on the total amount of sedimentary biologically stored polyP. Accordingly, P content in single large polyP granules is similar to multiple smaller inclusions in wider filaments. However, the presence of polyP stored in *Beggiatoa* at all depths supports the possibility for a biologically mediated sedimentary  $P_i$  release at the Peruvian Shelf as reported from other areas. A biological contribution to  $P_i$  fluxes was demonstrated in sediments near Barbados and from the Santa Monica basin by transcriptomic analyses (Jones et al., 2016). It was found that the expression of polyP related genes known to catalyze polyP formation and degradation was related to a release of  $P_i$  under anoxic conditions and an uptake under oxic conditions (Jones et al., 2016). Also the sulfur bacterium *Thiomargarita nambibiensis* was reported to degrade internally stored polyP inclusions with subsequent  $P_i$  release, which leads to extremely high pore water  $P_i$  concentrations resulting in the precipitation of hydroxyapatite in the Benguela upwelling system off the Namibian coast (Schulz & Schulz, 2005, Goldhammer et al., 2010). The formation of such high amounts of intracellular polyP is normally attributed to a luxury  $P_i$  uptake mechanism when excess  $P_i$  is available. This is well studied in waste water treatment plants and has been also regularly applied in environmental studies explaining  $P_i$  release. As mentioned earlier, polyP cycling is thought to be heavily influenced by prevailing redox conditions. Especially for *Beggiatoa* it has been shown that extracellular  $P_i$  is converted to PolyP under oxic and low sulfide conditions, leading to high intracellular P content present as polyP. In contrast, high sulfidic and anoxic conditions lead to a degradation of the internal polyP pool and a release of  $P_i$  to the extracellular environment (Figure 23, Brock & Schulz-Vogt, 2011).

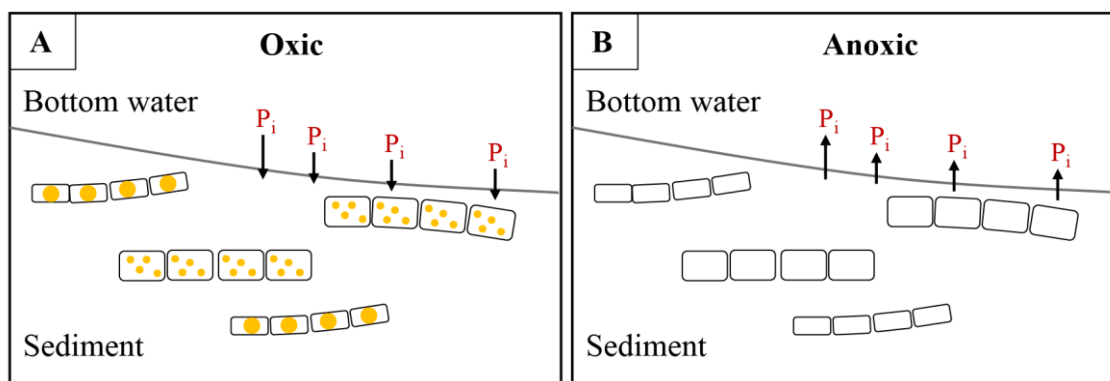


**Figure 23:** Current understanding of polyP cycling in sediments. A:  $P_i$  uptake and the formation of polyP during oxic conditions; B: polyP degradation and  $P_i$  release into the extracellular environment during anoxic conditions.

In light of the redox dependency of polyP formation and the different oxygen concentrations present at the respective depths (Table 5), the stable and comparable pool of polyP stored by *Beggiatoa* across the sampled depths is surprising, if expecting high polyP content under oxic conditions and low polyP under anoxic conditions. Oxygen concentrations in *Beggiatoa* mats were found to be  $10 \mu\text{M}$  with fully oxidized overlaying bottom water (Jørgensen & Revsbech, 1983). Since oxygen concentrations in bottom water of the Peruvian shelf were close to zero or completely depleted (Table 1), *Beggiatoa* filaments were likely limited in oxygen, despite their need for micro-aerobic growth conditions, which could also explain the low filament biovolumes. Rather, according to the current understanding of polyP cycling, the prevailing conditions would predominantly support polyP degradation with subsequent sedimentary  $P_i$  release being reflected in the actual observed  $P_i$  release rates and the possible relative contribution from *Beggiatoa* as discussed below.

The relatively uniform concentrations of  $P_i$ -equiv. in polyP are contrasted by the measured sedimentary  $P_i$  release rates (Figure 24, Lomnitz et al., unpublished). Fluxes showed considerable differences across depths and were highest at 77 m depth with a subsequent sharp decrease at 200 m and 244 m. In combination with the uniform intracellular polyP content of analyzed *Beggiatoa* filaments, relative contributions of biologically mediated sedimentary  $P_i$  release substantially differ with depth caused by pronounced differences in measured total  $P_i$  fluxes. (Figure 24).

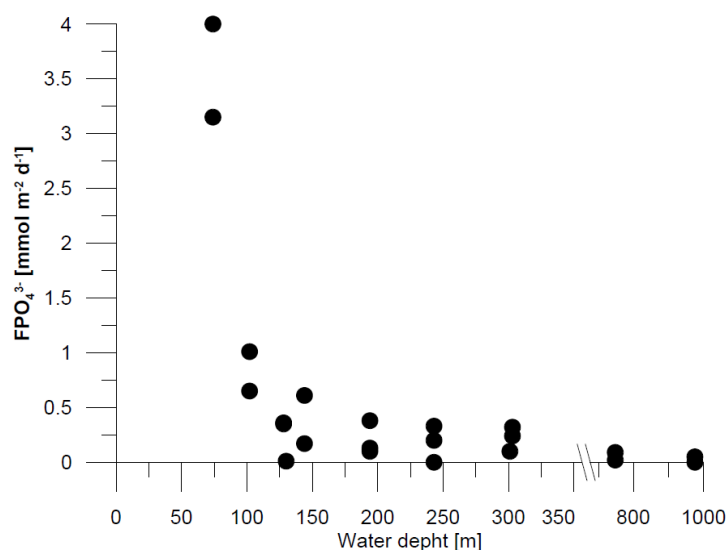


**Figure 24:** Phosphate fluxes across the Peruvian shelf (Lomnitz et al., unpublished).

Fluxes between  $3 - 4 \text{ mmol} \cdot \text{m}^{-2} \cdot \text{d}^{-1}$  ( $= 300 - 400 \text{ nmol} \cdot \text{cm}^{-2} \cdot \text{d}^{-1}$ ) at 77 m would deplete the stored P pool of around  $9 \text{ nmol} \cdot \text{cm}^{-3}$  in *Beggiatoa* (Figure 14) within 90 min if not in steady state and not permanently regenerated. If constantly regenerated, degradation of stored polyP would account for 2 -3% to the total sedimentary  $\text{P}_i$  flux (Table 6) at 77 m depth. In contrast to this,  $\text{P}_i$  release from polyP degradation from *Beggiatoa* at 200 m and 244 m depth could substantially contribute to the sedimentary  $\text{P}_i$  fluxes. A contribution of 24% as found at 200 m depth, would be twice as high as attributed to bacteria in Effingham Inlet (Sannigrahi & Ingllall, 2005) and would represent an important source of  $\text{P}_i$  to bottom waters. Therefore, polyP degradation with subsequent  $\text{P}_i$  release by *Beggiatoa* would potentially contribute a large fraction to the observed  $\text{P}_i$  fluxes measured, despite to low oxygen conditions. This would in particular be a prominent factor if the *Beggiatoa* mediated fluxes could be maintained and thus, the internal polyP pool would continuously be regenerated. According to the current understanding of polyP cycling at least transient oxic conditions would be required. The capacity to alternate between  $\text{P}_i$  uptake and  $\text{P}_i$  release makes these filaments “P capacitors” (Dale et al., 2013), which is especially important in systems with dynamic redox conditions as for example at the Peruvian upwelling system (Gutiérrez et al., 2008).

**Table 6:** Maximum relative contribution of *Beggiatoa* filaments to measured in situ  $P_i$  release and time until the polyP pool would be depleted if not continuously regenerated. Calculation with  $P_i$  fluxes from Figure 24 ( $3500 \mu\text{mol}\cdot\text{m}^{-2}\cdot\text{d}^{-1}$  in 77 m;  $250 \mu\text{mol}\cdot\text{m}^{-2}\cdot\text{d}^{-1}$  in 200 m and 244 m).

Depth	Time until depletion [min]	Potential relative contribution of $P_i$ in polyP to $P_i$ fluxes
77 m	107	3%
77 m	91	3%
77 m	85	2%
200 m	878	24%
200 m	744	21%
244 m	894	25%
244 m	1322	37%
244 m	2253	63%

The combination of the presence of polyP in large sulfur bacteria together with observed  $P_i$  release potentially mediated by bacteria, indicates the presence of a background sedimentary polyP pool, even under the not optimal very low oxygen conditions. The relative contribution reported above should also only be regarded as maximum estimates, since a very fast and complete regeneration of the polyP pool would be required. Therefore, it is likely that the  $P_i$  flux caused by polyP degradation in *Beggiatoa* contributes only a part to all responsible mechanisms.

Alternative sources of  $P_i$  release are particularly important at 77 depth, where the bacterial sources can only explain a maximum of 3 – 4%. Reductive dissolution of ironhydroxides under anoxic conditions with concomitant  $P_i$  release would be one prominent mechanisms, however, does not play an important role in Peruvian sediments, predominantly caused by the widely distributed anoxic water column preventing accumulation of oxidized ironhydroxids (Noffke et al., 2012, Lomintz et al., 2016). Preferential mineralization of P from particulate organic matter could be another sedimentary P source, but is also not considered to be relevant in the Peruvian upwelling system (Lomnitz et al., 2016). Altogether, it is possible that the large gap in the constructed P budget can for the most part be explained by  $P_i$  release from polyP storing *Beggiatoa*. However, more detailed analyses about the

prevailing polyP mechanisms are needed, since a pure dependence on redox conditions doesn't go far enough and does not explain the high biologically mediated contribution to sedimentary  $P_i$  release.

As mentioned above, the presence of polyP in *Beggiatoa* associated with a continuous release of  $P_i$  during nearly anoxic conditions requires a continuous regeneration of the polyP pool to not be depleted within a short time period. PolyP quantification revealed that the polyP pool in *Beggiatoa* was not fully depleted and still may contribute to observed  $P_i$  fluxes, even under anoxic conditions. Also a study by Hupfer & Rube in 2004 analyzing an array of lake sediments demonstrated the presence of polyP at most stations irrespective if the overlain water was oxic or anoxic. In addition, also the determined high  $P_i$  fluxes in Namibian sediments have to be in steady state for at least 3 months to explain the observed sedimentary precipitated hydroxyapatite (Schulz & Schulz, 2005). Therefore, also in these cases a continuous regeneration of polyP has to take place and shows that despite anoxic conditions not the complete polyP gets depleted and has to be continuously regenerated. This argues for an important role of polyP also under anoxic conditions as shown in the following.

### 4.3 Visualization of an active intracellular polyP pool

Phosphorus (P) has more than 23 isotopes with masses ranging from 24 u to 46 u including the stable P isotope  $^{31}\text{P}$ . The presence of only one stable isotope makes this element fundamentally different to N or C with each two ( $^{14}\text{N}$ ,  $^{15}\text{N}$  and  $^{12}\text{C}$ ,  $^{13}\text{C}$ ) different stable isotopes enabling stable isotope studies with nanoSIMS analyses and conclusions on microbial activity (Musat et al., 2012). Also the radioactive isotopes  $^{32}\text{P}$  and  $^{33}\text{P}$  are suited as biochemical tracers in isotope studies, in contrary to all other P isotopes caused in their short half-life time (Karl, 2014). In contrast to P, oxygen has three stable isotopes ( $^{16}\text{O}$  –  $^{18}\text{O}$ ), of which  $^{16}\text{O}$  is the most abundant one with > 99.7 atom% followed by  $^{17}\text{O}$  (~ 0.03 atom%) and  $^{18}\text{O}$  (0.205 atom%) (Meija et al., 2013). The abundance of more than one stable O isotope opens the possibility to conclude on different biogeochemical pathways involving  $P_i$ , based on analyses of  $^{18}\text{O}$  in  $P_i$ . The experiments conducted with the cultured strain *Beggiatoa* sp. 35Flor were meant as a proof of principle to show that  $^{18}\text{O}$  labeled water in combination with an enzyme mediated oxygen isotope exchange can be used to trace metabolic activity in oxygen rich molecules like polyP. The  $^{18}\text{O}$  enrichments present in Figure 15 demonstrate the formation of  $^{18}\text{O}$  labeled compounds during both oxic and anoxic incubation conditions under



both high and low sulfide fluxes.  $^{18}\text{O}$  enrichments through oxygen isotope exchange by breaking the covalent phosphoanhydride bonds can exclusively be mediated by enzymatic activity (Tudge, 1960, Longinelli, 1976), which is synonymous for biological activity (Blake et al., 2001, Figure 25).

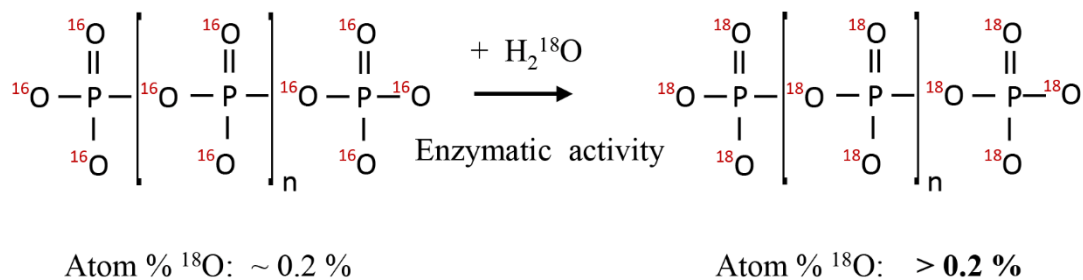
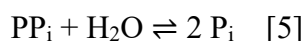


**Figure 25:** Hypothesized effect of enzyme mediated oxygen isotopes exchange when incubated with  $^{18}\text{O}$ -labelled water.  $^{18}\text{O}$  enrichments in polyP above the natural abundance of 0.2% is attributed to enzymatic activity.

The enzyme mediated oxygen isotope exchange is supported by low  $^{18}\text{O}$  enrichments in the cooled control (Figure 19) related to the temperature dependency of enzyme activity (Peterson et al., 2007). Only enzymatic activity can lead to  $^{18}\text{O}$  enrichments in polyP demonstrating the metabolic use of the energetic molecule. However, it is questionable which enzymes were responsible. One possibility would be the incorporation of  $^{18}\text{O}$  labeled  $\text{P}_i$  during polyP synthesis. Since almost fully labeled  $^{18}\text{O}$ -water (97 atom%) was directly injected to the *Beggiatoa* sp. mat at the oxic/ anoxic interface (Figure 5), it is likely that the metabolic water of the filaments was substantially composed of  $^{18}\text{O}$ -water. Oxygen isotope exchange between oxygen in water and oxygen in the reactant particularly occurs during hydrolysis reactions (Cohn, 1949; Liang & Blake, 2006; von Sperber et al., 2014). One example is the hydrolysis reaction mediated by the ubiquitous pyrophosphatase (PPase, reaction 5). This leads to a complete exchange of all four oxygen atoms in  $\text{P}_i$  within several hours. Consequently, this enzyme dominates  $^{18}\text{O}$  signatures in  $\text{P}_i$  in most aquatic systems (Boyer, 1978; Sperber et al., 2017; Blake et al., 1997; 2005).



Since all  $\text{P}_i$  ions present in the cytoplasm are involved into PPase mediated reactions (Blake et al., 2005), it is likely that a large fraction of intracellular  $\text{P}_i$  was at least partly labeled with  $^{18}\text{O}$  after the 24 h incubation time. A prolongation of existing polyP chains with  $^{18}\text{O}$  labeled

$P_i$  mediated by PPKs would thus lead to the observed  $^{18}\text{O}$  enrichments found in polyP after nanoSIMS analyses (Figure 26).

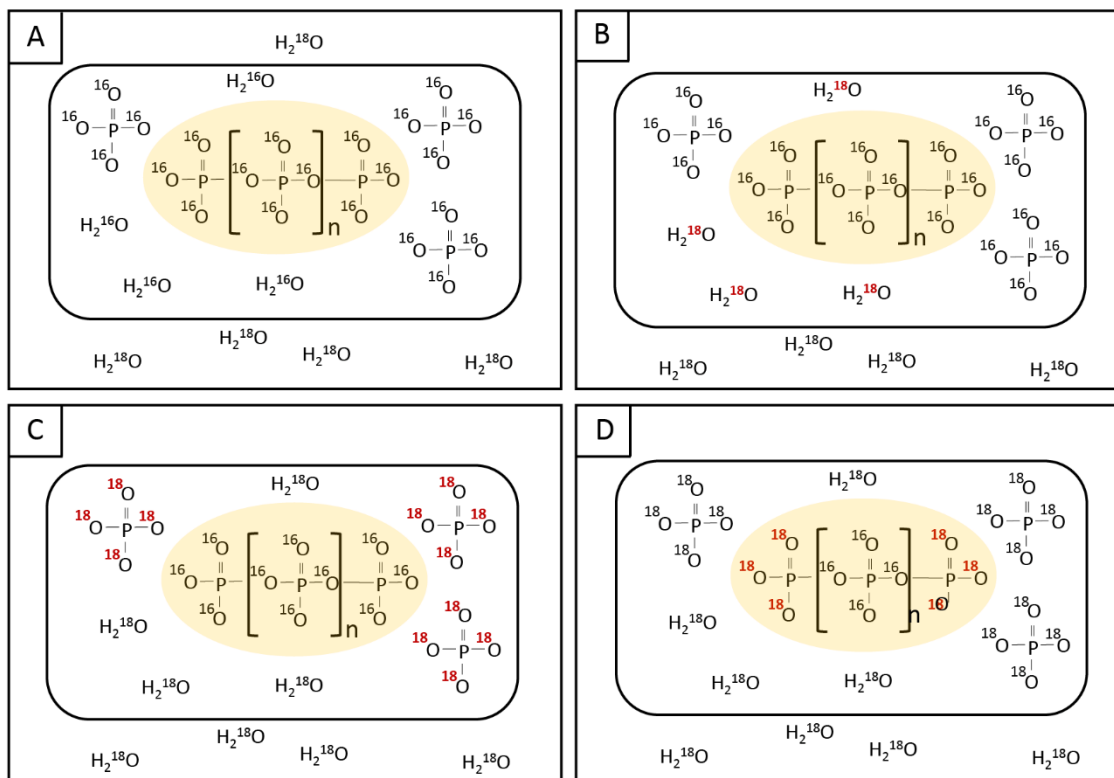


**Figure 26:** Conceptual model showing one possible way for  $^{18}\text{O}$  labeling of polyP. A: Oxygen is initially present as  $^{16}\text{O}$ , both in water and  $P_i$ /polyP. B: After the addition of highly labelled  $^{18}\text{O}$  water to the *Beggiatoa* mat, labelled water diffuses into the cytoplasm. C: Activity of PPase leads to a fully exchange of oxygen atoms in  $P_i$ . D: PPK adds  $^{18}\text{O}$  labelled  $P_i$  to polyP chains leading to  $^{18}\text{O}$  enrichments in polyP.

If PPK would be the dominant enzyme,  $^{18}\text{O}$  enrichments would increase with time as the relative proportion of  $P_i$  residues being composed of  $^{18}\text{O}$  isotopes increases. This would theoretically lead to an enrichment of up to 100 atom% if new polyP chains would be synthesized. Alternatively, polyP labeling with  $^{18}\text{O}$  could also occur during the degradation of polyP chains, which is considered to be predominantly mediated by PPX (reaction 4, Akiyama et al., 1993, Kulaev & Kulakovskaya, 2000) and considered to be related to a release of  $P_i$  into the extracellular environment (Brock & Schulz-Vogt, 2011). An oxygen isotope exchange during this hydrolysis reaction would thus lead to  $^{18}\text{O}$  labeling in the terminal phosphate residues of polyP chains. Therefore,  $^{18}\text{O}$  enrichments would be higher in shorter polyP chains (Table 7).

**Table 7:** Expected  $^{18}\text{O}$  enrichment in polyP with PPX as the dominate enzyme leading to exclusively  $^{18}\text{O}$  enriched terminal  $\text{P}_i$  residues.

$\text{P}_i$ residues in polyP	Enrichment $^{18}\text{O}$
3	66.6 atom%
10	20 atom%
50	4 atom%
100	2 atom%
1000	0.2 atom%

Enrichments reached maximum values between 2 – 4 atom% (Table 2), which would correspond to polyP chain lengths of 50 – 100  $\text{P}_i$  residues if only the terminal  $\text{P}_i$  residues would contain  $^{18}\text{O}$  labeled  $\text{P}_i$ . Since polyP chain length varies between three orders of magnitude ( $10^1$  –  $10^3$   $\text{P}_i$  residues, Kornberg et al., 1999), it would be necessary to determine the exact chain length of polyP to make final conclusions about the dominant enzymes being responsible for  $^{18}\text{O}$  enrichments, for example by Raman spectroscopy.

Substantial  $^{18}\text{O}$  enrichments were not only found in P rich areas defined as polyP, but also in the cytoplasm, especially during low sulfide incubations (Figure 19). Preparation for nanoSIMS analysis includes drying of sample, sputtering with a golden layer and measuring in a vacuum, thus strong mechanical forces are applied to the sample. Therefore, liquid compounds are not considered during nanoSIMS analysis and results obtained originated exclusively from solid compounds. Cellular dry weight is composed to a large fraction of 55% by proteins (Neidhardt et al., 1990), which can serve as a marker for metabolic activity (Hatzenpichler et al., 2014). Since oxygen isotope exchange also occurs at amino acids forming proteins (Springson & Rittenberg, 1951, Ye et al., 2009), the observed enrichments in the cytoplasm indicate ongoing standard metabolic processes like the synthesis of proteins. The pronounced differences in  $^{18}\text{O}$  enrichments present in the cytoplasm between filaments exposed to low and high sulfide fluxes and incubated under oxic conditions, indicate different physiological conditions prevailing in filaments during the respective treatments. Since the cytoplasm of filaments exposed to high sulfide fluxes was equally low enriched with  $^{18}\text{O}$  than the metabolically inactive control, standard metabolic processes, expressed as  $^{18}\text{O}$  enrichments in the cytoplasm, were drastically reduced during the exposure to high sulfide

fluxes. Considering that sulfide serves as the electron donor in the standard metabolism of *Beggiatoa* sp. (Reaction 6, Winogradsky, 1987, Nelson et al., 1983), it is remarkable that the general metabolism was impaired during both oxic and anoxic incubation conditions, caused by sulfide. It shows that even in the presence of oxygen, sulfide concentrations exceeded the oxygen concentrations needed to oxidize all sulfide present, which lead to an accumulation of stressfully high sulfide concentrations.



These unfavorable conditions are here reflected by low  $^{18}\text{O}$  enrichments in the cytoplasm, but can also be inferred from the intracellular sulfur content. It was shown that *Beggiatoa* sp. 35Flor can switch to sulfur respiration in the absence of oxygen concomitantly with an oxidation of intracellularly stored polyhydroxyalkanoates (PHA) (Schwedt et al., 2012). The low sulfur counts present in filaments exposed to high sulfide fluxes and incubated under anoxic conditions (Figure 21) support that adverse conditions prevailed. However, high sulfur content during the oxic incubation demonstrates an improved stress tolerance against high sulfide fluxes with oxygen being present. A different picture prevailed in filaments exposed to low sulfide concentrations, where sulfur content did not differ between the different treatments (Figure 20). It shows that filaments were not limited in oxygen since filaments did not switch to sulfur respiration. In addition,  $^{18}\text{O}$  enrichments in the cytoplasm were significantly higher after oxic and anoxic incubations compared to the inactive control. This underlines the presence of a general metabolic activity also during the energetically unfavorable anoxic incubation condition. It shows that sulfide levels were not high enough to trigger a stress response in the cells, either by sulfur respiration or a reduction of metabolic processes. This demonstrates that a general metabolism was active, which was able to be maintained also under these energetically unfavorable conditions (Langer et al., 2018).

Despite filaments exposed to high sulfide fluxes were impaired in their standard metabolic processes, polyP was highest enriched in the oxic incubation under these conditions (Table 2). This suggests a fundamental physiological role of polyP under these stressful conditions. The relative importance of polyP is also underlined when comparing the ratio between the means of enrichments in polyP and the cytoplasm (Table 4). This shows that elevated sulfide concentrations lead to a restriction of metabolic activity at polyP, which is supported when comparing filaments exposed to low sulfide concentrations where the relative importance of polyP is less pronounced. The increased importance of polyP during unfavorable conditions

presumably goes hand in hand with an increased activity of enzymes related to polyP metabolisms. An upregulation of PPK was for example shown in P stressed cultures of the marine diatom *Thalassiosira pseudonana*. (Dyhrman et al., 2012). Thus, polyP seems to have a pivotal role against stressfully environmental conditions which, besides from P limitation, can potentially be induced by several factors. One example is the exposure to high sulfide concentrations resulting in a release of  $P_i$  from polyP degradation. This was shown for *Beggiatoa* sp. 35Flor as a response mechanism to tolerate high sulfide concentrations when no suitable electron acceptor was present (Brock & Schulz-Vogt, 2011). Another stimulus could be energy-limited environments, in which polyP was proposed to function as an energy reservoir to maintain cellular integrity, as proposed for *Sulfurimonas* spp., which is a dominant microorganisms at pelagic redox clines (Möller et al., 2018). However, the often proposed function of PolyP as a substitute for ATP under energetically unfavorable conditions is arguable, since a comparable turnover time of the two energy carriers would be needed. Since the turnover time of ATP is substantially faster than the turnover time of polyP it could be only replaced for a maximum of two minutes, which was shown for *E.coli* in stationary phase (Chapman & Atkinson, 1977; Kornberg et al., 1999). Thus, polyP has most likely a more regularly role (Docampo et al., 2005), which can be vital during environmental stress.

The general metabolic importance of polyP, not only during stressful condition, are supported by the presence of significant  $^{18}O$  enrichments above the natural background in polyP irrespective of the treatment. This indicates a pivotal role of polyP also during favorable growth conditions, which is connected to a vital intracellularly recycling of polyP. NanoSIMS analyses were conducted after filaments were grown for seven days (see  $H_2O$  incubation of *Beggiatoa* strain 35 Flor M&M), which lead to a depletion of  $P_i$  in the external medium (Brock & Schulz-Vogt, 2011). Since labelled water was added after seven days, enrichments in polyP, which are synonymous with enzymatic activity of polyP related enzymes, do not originate from polyP chain length prolongation with  $P_i$  from the external medium being fully labelled with  $^{18}O$  established by PPase (section 4.1.1). According to the hitherto understanding of polyP cycling, one would expect a more inactive polyP pool, which cannot be increased due to a lack of available external  $P_i$ . However, polyP was significantly enriched, possibly at the end residue of polyP (section 4.1.1) showing a continuous involvement of polyP enzymes in metabolic processes, also during favorable oxic growth conditions. Thus, the enrichments in polyP indicating enzymatic activity originate from an

intense intracellular recycling of  $P_i$ . This is presumably mediated by PPK connecting the energetic P pools of ATP and polyP (Langer et al., 2018). Consequently, polyP utilization is not only strengthened during unfavorable environmental conditions, but is highly relevant also under oxic conditions. Therefore, polyP does not necessarily represent a “silent” P pool or serves only as an auxiliary metabolism as assumed for polyP metabolism for *Thiomargarita namibiensis* (Schulz & Schulz, 2005), or assumed from widely accepted polyP cycling models. Furthermore, the equivalent importance of polyP under oxic and anoxic conditions is underlined by similar intense P counts by nanoSIMS under both conditions (Figure 15). This is in contrast to sulfur, which intensities depend on environmental conditions (see above). The constant levels of polyP inferred from nanoSIMS counts in combination with indications on a highly mobile and enzymatically used polyP pool inferred from  $^{18}O$  enrichments argues for a stable level of polyP related enzymes. Laboratory experiments conducted with *E.coli* showed a constant level of polyP enzymes during the cell cycle which involved accumulation of large amounts of polyP (Rao et al., 1998). Interestingly, high accumulation of polyP was observed during  $P_i$  starvation, similar to results obtained by Dyhrman et al., 2012, where P was reallocated to polyP in the absence of  $P_i$ . Since external  $P_i$  was not available for filaments during  $^{18}O$  incubation, the observed enrichments under oxic incubation could hint to similar P limited conditions.

## 5 Conclusion and Outlook

The relevance of polyP for global and local P cycling has been often neglected, which lead to the perception of polyP as a “forgotten molecule” (Kornberg et al., 1995). The lack of studies dealing with polyP is mainly grounded in overall challenges in polyP research. This ranges from inadequate quantification methods to limited possibilities for getting insights into cellular P cycling, because of the presence of only one stable P isotope. Within this thesis I aimed to add insights about the quantity of polyP in coastal and marine environments and established a method enabling the visualization of O rich compounds like polyP to get insight about cellular activity of polyP.

PolyP quantification revealed a permanent presence of a background cellular polyP content in all analysed samples, irrespective if from pelagic bacteria from waters of the coastal Baltic Sea, from waters originating from the upwelling area off Peru, or in large sulfur bacteria attributed to the genus *Beggiatoa* spp. in sediments off Peru. Analysis of polyP in the latter confirms that these bacteria might contribute to the observed sedimentary  $P_i$  fluxes repeatedly observed in these sediments (Noffke et al., 2012, Lomnitz et al., 2016). The overall low oxygen content in these bottom waters has most likely supported the degradation of polyP with subsequent  $P_i$  release as reported from other marine anoxic sediments inferred from  $P_i$  flux measurements (Schulz & Schulz, 2005) or metatranscriptomic analyses (Jones et al., 2015). The high potential contribution of these filaments to observed  $P_i$  fluxes is also reflected in very big sized intracellular polyP inclusions. These were found in filaments with relatively small filament diameter representing the largest polyP granules found in the environment similar to those reported from the cultured strain *Beggiatoa* sp. 35Flor (Brock et al., 2012). The results obtained from quantification of polyP in bacteria from a coastal area of the Baltic Sea do not support a relevant role of polyP for the local P cycle as for example reported from the Sargasso Sea (Martin et al., 2014). Nevertheless, the continuous presence of polyP in all samples strongly argues for a permanent need of this inorganic molecule for basic metabolic processes. This can be inferred from results obtained after incubation of *Beggiatoa* sp. 35Flor with  $^{18}O$  water and subsequent nanoSIMS analysis. A permanent activity of polyP related enzymes was found, both during favourable and stressful growth conditions. Therefore, polyP is also heavily recycled and actively used also during favourable growth conditions and not an inactive P reservoir in oxygenated environments as often assumed. Enzyme activity was restricted to polyP related enzymes during anoxic high sulfide

conditions. This is in line with findings of extensive polyP utilization during exposure to high sulfide (Brock & Schulz-Vogt et al., 2011) and underlining the importance of polyP for cellular processes.

The newly established nanoSIMS method opens great possibilities to assess the activity of polyP related enzymes in different environments. Ex situ incubations of *Beggiatoa* spp. filaments showed the applicability for field samples, but also the need for preliminary experiments to find the correct tracer concentration for meaningful results. A simultaneously analysis of samples by Raman spectroscopy to determine polyP chain length would provide valuable information about the prevailing polyP enzymes being involved. The large polyP granules determined in *Beggiatoa* spp., and the permanent presence of polyP in bacteria also from coastal waters of the Baltic Sea shows the large potential for bacterial mediated  $P_i$  release in environments with changing redox conditions. The new insights about polyP quantities in different environments together with the now feasible visualization of the activity of polyP related enzymes expands the understanding of polyP and opens new possibilities for future research.



---

## References

- Achbergerová L, Nahálka J (2011) Polyphosphate-an ancient energy source and active metabolic regulator. *Microbial cell factories* 10:63.
- Akiyama M, Crooke E, Kornberg A (1993) An exopolyphosphatase of *Escherichia coli*. The enzyme and its ppx gene in a polyphosphate operon. *The Journal of biological chemistry* 268:633–639.
- Albuquerque JP de, Keim CN, Lins U (2010) Comparative analysis of *Beggiatoa* from hypersaline and marine environments. *Micron (Oxford, England 1993)* 41:507–517.
- Arning ET, Birgel D, Schulz-Vogt HN, Holmkvist L, Jørgensen BB, Larson A, Peckmann J (2008) Lipid Biomarker Patterns of Phosphogenic Sediments from Upwelling Regions. *Geomicrobiology Journal* 25:69–82.
- Arntz WE, Tarazona J, Gallardo VA, Flores LA, Salzwedel H (1991) Benthos communities in oxygen deficient shelf and upper slope areas of the Peruvian and Chilean Pacific coast, and changes caused by El Niño. *Geological Society, London, Special Publications* 58:131–154.
- Aschar-Sobbi R, Abramov AY, Diao C, Kargacin ME, Kargacin GJ, French RJ, Pavlov E (2008) High sensitivity, quantitative measurements of polyphosphate using a new DAPI-based approach. *Journal of fluorescence* 18:859–866.
- Ask J, Rowe O, Brugel S, Strömberg M, Byström P, Andersson A (2016) Importance of coastal primary production in the northern Baltic Sea. *Ambio* 45:635–648.
- Ault-Riché D, Fraley CD, Tzeng C-M, Kornberg A (1998) Novel Assay Reveals Multiple Pathways Regulating Stress-Induced Accumulations of Inorganic Polyphosphate in *Escherichia coli*. *Journal of bacteriology* 180:1841–1847.
- Azzoni R, Giordani G, Viaroli P (2005) Iron–sulphur–phosphorus Interactions: Implications for Sediment Buffering Capacity in a Mediterranean Eutrophic Lagoon (Sacca di Goro, Italy). *Hydrobiologia* 550:131–148.
- Björkman KM (2014) Polyphosphate goes from pedestrian to prominent in the marine P-cycle. *Proceedings of the National Academy of Sciences of the United States of America* 111:7890–7891.
- Blake RE (2005) Biogeochemical cycling of phosphorus: Insights from oxygen isotope effects of phosphoenzymes. *American Journal of Science* 305:596–620.
- Blake RE, Alt JC, Martini AM (2001) Oxygen isotope ratios of PO<sub>4</sub>: an inorganic indicator of enzymatic activity and P metabolism and a new biomarker in the search for life.

- Proceedings of the National Academy of Sciences of the United States of America 98:2148–2153.
- Blake RE, O'neil JR, Garcia GA (1997) Oxygen isotope systematics of biologically mediated reactions of phosphate: I. Microbial degradation of organophosphorus compounds. *Geochimica et Cosmochimica Acta* 61:4411–4422.
- Bohne B, Bohne K (2008) Monitoring zum Wasserhaushalt einer auf litoralem Versumpfungsmoor gewachsenen Regenmoorkalotte - Beispiel Naturschutzgebiet "Hütelmoor" bei Rostock. In: *Aspekte der Geoökologie*; Weißensee Verlag.
- Boyer PD (1978) Isotope exchange probes and enzyme mechanisms. *Acc. Chem. Res.* 11:218–224.
- Braun PD, Schulz-Vogt HN, Vogts A, Nausch M (2018) Differences in the accumulation of phosphorus between vegetative cells and heterocysts in the cyanobacterium *Nodularia spumigena*. *Scientific reports* 8:5651.
- Brock J, Rhiel E, Beutler M, Salman V, Schulz-Vogt HN (2012) Unusual polyphosphate inclusions observed in a marine *Beggiatoa* strain. *Antonie van Leeuwenhoek* 101:347–357.
- Brock J, Schulz-Vogt HN (2011) Sulfide induces phosphate release from polyphosphate in cultures of a marine *Beggiatoa* strain. *The ISME journal* 5:497–506.
- Brown MRW, Kornberg A (2004) Inorganic polyphosphate in the origin and survival of species. *Proceedings of the National Academy of Sciences of the United States of America* 101:16085–16087.
- Bunse C, Bertos-Fortis M, Sassenhagen I, Sildever S, Sjöqvist C, Godhe A, Gross S, Kremp A, Lips I, Lundholm N, Rengefors K, Seftom J, Pinhassi J, Legrand C (2016) Spatio-Temporal Interdependence of Bacteria and Phytoplankton during a Baltic Sea Spring Bloom. *Frontiers in microbiology* 7:517.
- Chapman AG, Atkinson DE (1977) Adenine Nucleotide Concentrations and Turnover Rates. Their Correlation with Biological Activity in Bacteria and Yeast. In: *Advances in Microbial Physiology Volume 15, Vol. 15*. Elsevier.
- Cho H-M, Kim G (2016) Determining groundwater Ra end-member values for the estimation of the magnitude of submarine groundwater discharge using Ra isotope tracers. *Geophys. Res. Lett.* 43:3865–3871.
- Cho H-M, Kim G, Kwon EY, Moosdorf N, Garcia-Orellana J, Santos IR (2018) Radium tracing nutrient inputs through submarine groundwater discharge in the global ocean. *Scientific reports* 8:2439.

- Cohn M (1949) Mechanisms of cleavage of glucose-1-phosphate. *The Journal of biological chemistry* 180:771–781.
- Cohn M (1958) Phosphate-water exchange reaction catalyzed by inorganic pyrophosphatase of yeast. *The Journal of biological chemistry* 230:369–379.
- Dale AW, Bertics VJ, Treude T, Sommer S, Wallmann K (2013) Modeling benthic–pelagic nutrient exchange processes and porewater distributions in a seasonally hypoxic sediment: evidence for massive phosphate release by *Beggiatoa*? *Biogeosciences* 10:629–651.
- Davelaar D (1993) Ecological significance of bacterial polyphosphate metabolism in sediments. *Hydrobiologia* 253:179–192.
- Davies CL, SurrIDGE BWJ, Goody DC (2014) Phosphate oxygen isotopes within aquatic ecosystems: Global data synthesis and future research priorities. *The Science of the total environment* 496:563–575.
- Diaz J, Ingall E, Benitez-Nelson C, Paterson D, Jonge MD de, McNulty I, Brandes JA (2008) Marine polyphosphate: a key player in geologic phosphorus sequestration. *Science (New York, N.Y.)* 320:652–655.
- Diaz JM, Björkman KM, Haley ST, Ingall ED, Karl DM, Longo AF, Dyrman ST (2016) Polyphosphate dynamics at Station ALOHA, North Pacific subtropical gyre. *Limnol. Oceanogr.* 61:227–239.
- Diaz JM, Ingall ED (2010) Fluorometric quantification of natural inorganic polyphosphate. *Environmental science & technology* 44:4665–4671.
- Docampo R, Souza W de, Miranda K, Rohloff P, Moreno SNJ (2005) Acidocalcisomes - conserved from bacteria to man. *Nature reviews. Microbiology* 3:251–261.
- Dyrman S, Ammerman J, van Mooy B (2007) Microbes and the Marine Phosphorus Cycle. *Oceanogr.* 20:110–116.
- Dyrman ST, Jenkins BD, Rynearson TA, Saito MA, Mercier ML, Alexander H, Whitney LP, Drzewianowski A, Bulygin VV, Bertrand EM, Wu Z, Benitez-Nelson C, Heithoff A (2012) The transcriptome and proteome of the diatom *Thalassiosira pseudonana* reveal a diverse phosphorus stress response. *PloS one* 7:e33768.
- Ehlert C, Grasse P, Gutiérrez D, Salvattecchi R, Frank M (2015) Nutrient utilisation and weathering inputs in the Peruvian upwelling region since the Little Ice Age. *Clim. Past* 11:187–202.
- Einsele W (1936) Über die Beziehungen des Eisenkreislaufs zum Phosphatkreislauf im eutrophen See. *Arch. Hydrobiolog.* 29:664–686.

- Emsley J (2001) The 13th Element. *J. Chem. Educ.* 78.
- Freese HM, Görs S, Karsten U, Schumann R (2007) Dissolved inorganic nutrients and organic substrates in the River Warnow (North-Eastern Germany) – Utilisation by bacterioplankton. *Limnologica* 37:264–277.
- Gächter R, Meyer JS (1993) The role of microorganisms in mobilization and fixation of phosphorus in sediments. *Hydrobiologia* 253:103–121.
- Gallardo VA (1977) Large benthic microbial communities in sulphide biota under Peru–Chile Subsurface Countercurrent. *Nature* 268:331–332.
- Goldhammer T, Brüchert V, Ferdelman TG, Zabel M (2010) Microbial sequestration of phosphorus in anoxic upwelling sediments. *Nature Geosci* 3:557–561.
- Gutiérrez D, Enríquez E, Purca S, Quipúzcoa L, Marquina R, Flores G, Graco M (2008) Oxygenation episodes on the continental shelf of central Peru: Remote forcing and benthic ecosystem response. *Progress in Oceanography* 79:177–189.
- Hahn J, Köhler S, Glatzel S, Jurasinski G (2015) Methane Exchange in a Coastal Fen in the First Year after Flooding--A Systems Shift. *PloS one* 10:e0140657.
- Hanrahan G, Salmassi TM, Khachikian CS, Foster KL (2005) Reduced inorganic phosphorus in the natural environment: significance, speciation and determination. *Talanta* 66:435–444.
- Harold FM (1964) Enzymatic and genetic control of polyphosphate accumulation in *Aerobacter aerogenes*. *Journal of general microbiology* 35:81–90.
- Hatzenpichler R, Scheller S, Tavormina PL, Babin BM, Tirrell DA, Orphan VJ (2014) In situ visualization of newly synthesized proteins in environmental microbes using amino acid tagging and click chemistry. *Environmental microbiology* 16:2568–2590.
- Havelmeyer S (2013) Polyphosphate storage in the family *Beggiatoaceae* with a focus on the species *Beggiatoa alba* (Doctoral dissertation) Retrieved from: <https://elib.suub.uni-bremen.de/peid=D00103474>.
- Høgslund S, Revsbech NP, Kuenen JG, Jørgensen BB, Gallardo VA, van de Vossenberg J, Nielsen JL, Holmkvist L, Arning ET, Nielsen LP (2009) Physiology and behaviour of marine Thioploca. *The ISME journal* 3:647–657.
- Holmkvist L, Arning ET, Küster-Heins K, Vandieken V, Peckmann J, Zabel M, Jørgensen BB (2010) Phosphate geochemistry, mineralization processes, and Thioploca distribution in shelf sediments off central Chile. *Marine Geology* 277:61–72.
- Huettel M, Rusch A (2000) Transport and degradation of phytoplankton in permeable sediment. *Limnol. Oceanogr.* 45:534–549.

- Hupfer M, Gtichter R, Ruegger RR (1995) Polyphosphate in lake sediments:  $^{31}\text{P}$  NMR spectroscopy as a tool for its identification. *Limnol. Oceanogr.* 40:610–617.
- Hupfer M, Ruübe B, Schmieder P (2004) Origin and diagenesis of polyphosphate in lake sediments: A  $^{31}\text{P}$  NMR study. *Limnol. Oceanogr.* 49:1–10.
- Ishige K, Zhang H, Kornberg A (2002) Polyphosphate kinase (PPK2), a potent, polyphosphate-driven generator of GTP. *Proceedings of the National Academy of Sciences of the United States of America* 99:16684–16688.
- Janssen F, Huettel M, Witte U (2005) Pore-water advection and solute fluxes in permeable marine sediments (II): Benthic respiration at three sandy sites with different permeabilities (German Bight, North Sea). *Limnol. Oceanogr.* 50:779–792.
- Jean MRN, Gonzalez-Rizzo S, Gauffre-Autelin P, Lengger SK, Schouten S, Gros O (2015) Two new *Beggiatoa* species inhabiting marine mangrove sediments in the Caribbean. *PloS one* 10:e0117832.
- Jones DS, Flood BE, Bailey JV (2016) Metatranscriptomic insights into polyphosphate metabolism in marine sediments. *The ISME journal* 10:1015–1019.
- Jørgensen BB, Revsbech NP (1983) Colorless Sulfur Bacteria, *Beggiatoa* spp. and *Thiovulum* spp., in  $\text{O}_2$  and  $\text{H}_2\text{S}$  Microgradients. *Applied and environmental microbiology* 45:1261–1270.
- Jørgensen BB, Dunker R, Grünke S, Røy H (2010) Filamentous sulfur bacteria, *Beggiatoa* spp., in arctic marine sediments (Svalbard, 79 degrees N). *FEMS microbiology ecology* 73:500–513.
- Jurasinski G, Janssen M, Voss M, Böttcher ME, Brede M, Burchard H, Forster S, Gosch L, Gräwe U, Gründling-Pfaff S, Haider F, Ibenthal M, Karow N, Karsten U, Kreuzburg M, Lange X, Leinweber P, Massmann G, Ptak T, Rezanezhad F, Rehder G, Romoth K, Schade H, Schubert H, Schulz-Vogt H, Sokolova IM, Strehse R, Unger V, Westphal J, Lennartz B (2018) Understanding the Coastal Ecocline: Assessing Sea–Land Interactions at Non-tidal, Low-Lying Coasts Through Interdisciplinary Research. *Front. Mar. Sci.* 5:2473.
- Kalvelage T, Lavik G, Jensen MM, Revsbech NP, Löscher C, Schunck H, Desai DK, Hauss H, Kiko R, Holtappels M, LaRoche J, Schmitz RA, Graco MI, Kuypers MMM (2015) Aerobic Microbial Respiration In Oceanic Oxygen Minimum Zones. *PloS one* 10:e0133526.
- Kamp A, Røy H, Schulz-Vogt HN (2008) Video-supported analysis of *Beggiatoa* filament growth, breakage, and movement. *Microbial ecology* 56:484–491.

- Karl DM (2014) Microbially mediated transformations of phosphorus in the sea: new views of an old cycle. *Annual review of marine science* 6:279–337.
- Karl DM, Björkman KM (2015) Dynamics of Dissolved Organic Phosphorus. In: *Biogeochemistry of Marine Dissolved Organic Matter*. Elsevier.
- Karstensen J, Stramma L, Visbeck M (2008) Oxygen minimum zones in the eastern tropical Atlantic and Pacific oceans. *Progress in Oceanography* 77:331–350.
- Kolp O (1957) *Die Nordöstliche Heide Mecklenburgs*. VEB Deutscher Verlag Der Wissenschaften, Berlin.
- Kornberg A (1995) Inorganic polyphosphate: toward making a forgotten polymer unforgettable. *Journal of bacteriology* 177:491–496.
- Kornberg A, Kornberg SR, Simms ES (1956) Metaphosphate synthesis by an enzyme from *Escherichia coli*. *Biochimica et biophysica acta* 20:215–227.
- Kornberg A, Rao NN, Ault-Riché D (1999) Inorganic polyphosphate: a molecule of many functions. *Annual review of biochemistry* 68:89–125.
- Kotwicki L, Grzelak K, Czub M, Dellwig O, Gentz T, Szymczycha B, Böttcher ME (2014) Submarine groundwater discharge to the Baltic coastal zone: Impacts on the meiofaunal community. *Journal of Marine Systems* 129:118–126.
- Kraal P, Bostick BC, Behrends T, Reichart G-J, Slomp CP (2015) Characterization of phosphorus species in sediments from the Arabian Sea oxygen minimum zone: Combining sequential extractions and X-ray spectroscopy. *Marine Chemistry* 168:1–8.
- Kreuzburg M, Ibenthal M, Janssen M, Rehder G, Voss M, Naumann M, Feldens P (2018) Sub-marine Continuation of Peat Deposits From a Coastal Peatland in the Southern Baltic Sea and its Holocene Development. *Front. Earth Sci.* 6:309.
- Kulaev I, Kulakovskaya T (2000) Polyphosphate and phosphate pump. *Annual review of microbiology* 54:709–734.
- Kulakova AN, Hobbs D, Smithen M, Pavlov E, Gilbert JA, Quinn JP, McGrath JW (2011) Direct quantification of inorganic polyphosphate in microbial cells using 4'-6-diamidino-2-phenylindole (DAPI). *Environmental science & technology* 45:7799–7803.
- Kuroda A, Kornberg A (1997) Polyphosphate kinase as a nucleoside diphosphate kinase in *Escherichia coli* and *Pseudomonas aeruginosa*. *Proceedings of the National Academy of Sciences of the United States of America* 94:439–442.
- Kwon EY, Kim G, Primeau F, Moore WS, Cho H-M, DeVries T, Sarmiento JL, Charette MA, Cho Y-K (2014) Global estimate of submarine groundwater discharge based on an observationally constrained radium isotope model. *Geophys. Res. Lett.* 41:8438–8444.

- Langer S, Vogts A, Schulz-Vogt HN (2018) Simultaneous Visualization of Enzymatic Activity in the Cytoplasm and at Polyphosphate Inclusions in *Beggiatoa* sp. Strain 35Flor Incubated with  $^{18}\text{O}$ -Labeled Water. mSphere
- Levin L, Gutiérrez D, Rathburn A, Neira C, Sellanes J, Muñoz P, Gallardo V, Salamanca M (2002) Benthic processes on the Peru margin: a transect across the oxygen minimum zone during the 1997–98 El Niño. *Progress in Oceanography* 53:1–27.
- Liang Y, Blake RE (2006) Oxygen isotope signature of Pi regeneration from organic compounds by phosphomonoesterases and photooxidation. *Geochimica et Cosmochimica Acta* 70:3957–3969.
- Liebermann L (1888) Ueber das Nuclein der Hefe und künstliche Darstellung eines Nucleins aus Eiweiss und Metaphosphorsäure. *Ber. Dtsch. Chem. Ges.* 21:598–600.
- Lomnitz U, Sommer S, Dale AW, Löscher CR, Noffke A, Wallmann K, Hensen C (2016) Benthic phosphorus cycling in the Peruvian oxygen minimum zone. *Biogeosciences* 13:1367–1386.
- Longinelli A, Bartelloni M, Cortecchi G (1976) The isotopic cycle of oceanic phosphate, I. *Earth and Planetary Science Letters* 32:389–392.
- Mackenzie FT (ed) (2011) *Sediments, diagenesis, and sedimentary rocks*. Elsevier, Amsterdam, San Diego, CA.
- Martin P, Dyrman ST, Lomas MW, Poulton NJ, van Mooy BAS (2014) Accumulation and enhanced cycling of polyphosphate by Sargasso Sea plankton in response to low phosphorus. *Proceedings of the National Academy of Sciences of the United States of America* 111:8089–8094.
- Martin P, van Mooy BAS (2013) Fluorometric quantification of polyphosphate in environmental plankton samples: extraction protocols, matrix effects, and nucleic acid interference. *Applied and environmental microbiology* 79:273–281.
- McKay LJ, MacGregor BJ, Biddle JF, Albert DB, Mendlovitz HP, Hoer DR, Lipp JS, Lloyd KG, Teske AP (2012) Spatial heterogeneity and underlying geochemistry of phylogenetically diverse orange and white *Beggiatoa* mats in Guaymas Basin hydrothermal sediments. *Deep Sea Research Part I: Oceanographic Research Papers* 67:21–31.
- McMahon KD, Read EK (2013) Microbial contributions to phosphorus cycling in eutrophic lakes and wastewater. *Annual review of microbiology* 67:199–219.

- Meija J, Coplen TB, Berglund M, Brand WA, Bièvre P de, Gröning M, Holden NE, Irrgeher J, Loss RD, Walczyk T, Prohaska T (2016) Atomic weights of the elements 2013 (IUPAC Technical Report). *Pure and Applied Chemistry* 88:265–291.
- Meyer A (1904) Orientierende untersuchungen über verbreitung, Morphologie und chemie des volutins. *Botanische Zeitung* 69:113–152.
- Miegel, K., Graeff, T., Selle, B., Salzmann, T., Franck, C., Bronstert, A (2016) Untersuchung eines renaturierten Niedermooses an der mecklenburgischen Ostseeküste – Teil I: Systembeschreibung und hydrologische Grundcharakterisierung. *Hydrologie and Wasserbewirtschaftung* 4.
- Möller L, Laas P, Rogge A, Goetz F, Bahlo R, Leipe T, Labrenz M (2019) Sulfurimonas subgroup GD17 cells accumulate polyphosphate under fluctuating redox conditions in the Baltic Sea: possible implications for their ecology. *The ISME journal* 13:482–493.
- Mortimer CH (1941) The Exchange of Dissolved Substances Between Mud and Water in Lakes. *The Journal of Ecology* 29:280.
- Mosch T, Sommer S, Dengler M, Noffke A, Bohlen L, Pfannkuche O, Liebetrau V, Wallmann K (2012) Factors influencing the distribution of epibenthic megafauna across the Peruvian oxygen minimum zone. *Deep Sea Research Part I: Oceanographic Research Papers* 68:123–135.
- Musat N, Foster R, Vagner T, Adam B, Kuypers MMM (2012) Detecting metabolic activities in single cells, with emphasis on nanoSIMS. *FEMS microbiology reviews* 36:486–511.
- Neidhardt FC, Ingraham JL, Schaechter M (1990) *Physiology of the bacterial cell: a molecular approach*. Sinauer Associates, Sunderland, MA.
- Nelson DC, Jannasch HW (1983) Chemoautotrophic growth of a marine Beggiatoa in sulfide-gradient cultures. *Archives of microbiology* 136:262–269.
- Noffke A, Hensen C, Sommer S, Scholz F, Bohlen L, Mosch T, Graco M, Wallmann K (2012) Benthic iron and phosphorus fluxes across the Peruvian oxygen minimum zone. *Limnol. Oceanogr.* 57:851–867.
- Orchard ED, Benitez-Nelson CR, Pellechia PJ, Lomas MW, Dyrman ST (2010) Polyphosphate in *Trichodesmium* from the low-phosphorus Sargasso Sea. *Limnol. Oceanogr.* 55:2161–2169.
- Pasek MA, Sampson JM, Atlas Z (2014) Redox chemistry in the phosphorus biogeochemical cycle. *Proceedings of the National Academy of Sciences of the United States of America* 111:15468–15473.



- Paytan A, Kolodny Y, Neori A, Luz B (2002) Rapid biologically mediated oxygen isotope exchange between water and phosphate. *Global Biogeochemical Cycles* 16:13-1-13-8.
- Paytan A, McLaughlin K (2007) The oceanic phosphorus cycle. *Chemical reviews* 107:563–576.
- Pennington JT, Mahoney KL, Kuwahara VS, Kolber DD, Calienes R, Chavez FP (2006) Primary production in the eastern tropical Pacific: A review. *Progress in Oceanography* 69:285–317.
- Peterson ME, Daniel RM, Danson MJ, Eysenhard R (2007) The dependence of enzyme activity on temperature: determination and validation of parameters. *The Biochemical journal* 402:331–337.
- Polerecky L, Adam B, Milucka J, Musat N, Vagner T, Kuypers MMM (2012) Look@NanoSIMS--a tool for the analysis of nanoSIMS data in environmental microbiology. *Environmental microbiology* 14:1009–1023.
- Rao NN, Liu S, Kornberg A (1998) Inorganic polyphosphate in *Escherichia coli*: the phosphate regulon and the stringent response. *Journal of bacteriology* 180:2186–2193.
- Rao NN, Gómez-García MR, Kornberg A (2009) Inorganic polyphosphate: essential for growth and survival. *Annual review of biochemistry* 78:605–647.
- Rezanezhad F, Price JS, Quinton WL, Lennartz B, Milojevic T, van Cappellen P (2016) Structure of peat soils and implications for water storage, flow and solute transport: A review update for geochemists. *Chemical Geology* 429:75–84.
- Roden EE, Edmonds JW (1997) Phosphate mobilization in iron-rich anaerobic sediments: microbial Fe(III) oxide reduction versus iron sulfide formation. *Arch. Hydrobiol.*:347–378.
- Ruttenberg KC (2011) The Global Phosphorus Cycle. In: Mackenzie FT (ed) *Sediments, diagenesis, and sedimentary rocks*. Elsevier, Amsterdam, San Diego, CA.
- Salman V, Amann R, Girsch A-C, Polerecky L, Bailey JV, Høgslund S, Jessen G, Pantoja S, Schulz-Vogt HN (2011) A single-cell sequencing approach to the classification of large, vacuolated sulfur bacteria. *Systematic and applied microbiology* 34:243–259.
- Sannigrahi P, Ingall E (2005) Polyphosphates as a source of enhanced P fluxes in marine sediments overlain by anoxic waters: Evidence from <sup>31</sup>P NMR. *Geochemical Transactions* 6:52.
- Santoro AE (2010) Microbial nitrogen cycling at the saltwater–freshwater interface. *Hydrogeol J* 18:187–202.
- Schink B, Friedrich M (2000) Phosphite oxidation by sulphate reduction. *Nature* 406:37.

- Schulz HN, Jørgensen BB, Fossing HA, Ramsing NB (1996) Community Structure of Filamentous, Sheath-Building Sulfur Bacteria, *Thioploca* spp., off the Coast of Chile. *Applied and environmental microbiology* 62:1855–1862.
- Schulz HN, Strotmann B, Gallardo VA, Jørgensen BB (2000) Population study of the filamentous sulfur bacteria *Thioploca* spp. off the Bay of Concepción, Chile. *Mar. Ecol. Prog. Ser.* 200:117–126.
- Schulz HN, Schulz HD (2005) Large Sulfur Bacteria and the Formation of Phosphorite. *Science* 307:416–418.
- Schulz-Vogt HN, Pollehne F, Jürgens K, Arz HW, Beier S, Bahlo R, Dellwig O, Henkel JV, Herlemann DPR, Krüger S, Leipe T, Schott T (2019) Effect of large magnetotactic bacteria with polyphosphate inclusions on the phosphate profile of the suboxic zone in the Black Sea. *The ISME journal* 13:1198–1208.
- Schwedt A, Kreutzmann A-C, Polerecky L, Schulz-Vogt HN (2011) Sulfur respiration in a marine chemolithoautotrophic beggiatoa strain. *Frontiers in microbiology* 2:276.
- Skorko R (1989) Polyphosphate as a source of phosphoryl group in protein modification in the archaeobacterium *Sulfolobus acidocaldarius*. *Biochimie* 71:1089–1093.
- Solórzano L, Strickland JDH (1968) Polyphosphate in Seawater. *Limnol. Oceanogr.* 13:515–518.
- Sommer S, Gier J, Treude T, Lomnitz U, Dengler M, Cardich J, Dale AW (2016) Depletion of oxygen, nitrate and nitrite in the Peruvian oxygen minimum zone cause an imbalance of benthic nitrogen fluxes. *Deep Sea Research Part I: Oceanographic Research Papers* 112:113–122.
- Sperber C von, Kries H, Tamburini F, Bernasconi SM, Frossard E (2014) The effect of phosphomonoesterases on the oxygen isotope composition of phosphate. *Geochimica et Cosmochimica Acta* 125:519–527.
- Sperber C von, Lewandowski H, Tamburini F, Bernasconi SM, Amelung W, Frossard E (2017) Kinetics of enzyme-catalysed oxygen isotope exchange between phosphate and water revealed by Raman spectroscopy. *J. Raman Spectrosc.* 48:368–373.
- Springson D, RITTENBERG D (1951) Nature of the Activation Process in Enzymatic Reactions. *Nature* 167:484.
- Steinfeldt R, Sültenfuß J, Dengler M, Fischer T, Rhein M (2015) Coastal upwelling off Peru and Mauritania inferred from helium isotope disequilibrium. *Biogeosciences* 12:7519–7533.

- Stone BL, White AK (2012) Most probable number quantification of hypophosphite and phosphite oxidizing bacteria in natural aquatic and terrestrial environments. *Archives of microbiology* 194:223–228.
- Strub PT, Mesias, J. M., Montecino, V., Ontecino, R., and Salinas (eds) (1995) Coastal ocean circulation of western South America. Wiley, New York.
- Szymona M, Ostrowski W (1964) Inorganic polyphosphate glucokinase of *Mycobacterium phlei*. *Biochimica et Biophysica Acta (BBA) - Specialized Section on Enzymological Subjects* 85:283–295.
- Temperton B, Gilbert JA, Quinn JP, McGrath JW (2011) Novel analysis of oceanic surface water metagenomes suggests importance of polyphosphate metabolism in oligotrophic environments. *PLoS one* 6:e16499.
- Thilo E (1955) Die kondensierten Phosphate. *Angew. Chem.* 67:141–145.
- Tijssen JPF, Beekes HW, van Steveninck J (1982) Localization of polyphosphates in *Saccharomyces fragilis*, as revealed by 4',6-diamidino-2-phenylindole fluorescence. *Biochimica et Biophysica Acta (BBA) - Molecular Cell Research* 721:394–398.
- Tudge AP (1960) A method of analysis of oxygen isotopes in orthophosphate—its use in the measurement of paleotemperatures. *Geochimica et Cosmochimica Acta* 18:81–93.
- Voigtländer, U., Schmidt, J., Scheller, W. (1964) Pflege und Entwicklungsplan NSG. Heiligensee und Hütelmoor, Schwerin.
- White AK, Metcalf WW (2007) Microbial metabolism of reduced phosphorus compounds. *Annual review of microbiology* 61:379–400.
- Winogradsky S (1887) Ueber Schwefelbakterien. *Botanische Zeitung* 17.
- Yamagata Y, Watanabe H, Saitoh M, Namba T (1991) Volcanic production of polyphosphates and its relevance to prebiotic evolution. *Nature* 352:516–519.
- Ye X, Luke B, Andresson T, Blonder J (2009) <sup>18</sup>O stable isotope labeling in MS-based proteomics. *Briefings in functional genomics & proteomics* 8:136–144.
- Yoshida A (1955) Studies on metaphosphate: II. Heat of hydrolysis of metaphosphate extracted from yeast cells. *The Journal of Biochemistry* 42:163–168.
- Zhang H, Ishige K, Kornberg A (2002) A polyphosphate kinase (PPK2) widely conserved in bacteria. *Proceedings of the National Academy of Sciences of the United States of America* 99:16678–16683.

## List of Figures

Figure 1: Phosphate cycling in bacteria in aquatic environments. Dissolved $P_i$ can be taken up by free diffusion (1) or via membrane bound transport proteins (2a) after enzymatic mediated extracellular hydrolysis of organic P compounds (2). $P_i$ in the cytoplasm is subjected to an array of enzymatic processes leading to oxygen isotope exchange between water and phosphate (3), before it is incorporated into inorganic (e.g. polyphosphate) or organic (e.g. biomass) compounds (4). Metabolic processes or cell dead/ lysis lead to the release of intracellular P compounds (5), which can be taken up again ( $P_i$ , 6) or recycled through extracellular enzymes ( $P_{org}$ , 7). (Figure and content of description after Blake et al., 2005). .....	3
Figure 2: Linear polyP with variable length (n). .....	4
Figure 3: PolyP in bacteria stained with DAPI from an environmental sample (A) and in one <i>Beggiatoa</i> sp. 35Flor filament (B) discernible as yellow signals. ....	8
Figure 4: The study area of "Baltic Transcoast" with station numbers used for bottom-, ground-, and pore-water sampling for polyP quantification. ....	12
Figure 5: <i>Beggiatoa</i> filaments visible as a white mat situated at the oxic / anoxic interface between oxygen fluxes from the top and sulfide fluxes from the bottom. $H_2^{18}O$ was directly inoculated into the mat after 7 days of growth. ....	16
Figure 6: Concentrations of $P_i$ -equiv. in polyP in bottom water samples at different stations during different months in 2016. ....	19
Figure 7: Concentrations of $P_i$ -equiv. in polyP in porewater sampled at the beach. ....	20
Figure 8: Mean Concentrations of $P_i$ -equiv. in polyP in groundwater from two wells. GW2 was sampled in April, September and December (A). B shows concentrations sampled in December from both GW1 and GW2. ....	21
Figure 9: Means of $P_i$ -equiv. in polyP in the pelagic zone of the continental shelf off Peru at stations situated at water depths of 128 m (A) and 244 m (B). ....	22
Figure 10: DAPI stained filaments of the family <i>Beggiatoaceae</i> with differently sized polyP inclusions. A + C: Big polyP inclusions in relatively small filaments with a diameter between 4 and 5 $\mu m$ ; B + D: Small polyP inclusions in relatively big filaments with diameters between 12 and 15 $\mu m$ . ....	23
Figure 11: Means of filament counts from a minimum of five subsamples per $cm^3$ sediment at stations with maximum water depth of 77 m, 200 m and 244 m. ....	24
Figure 12: Relative abundances of filament diameter distribution of <i>Beggiatoa</i> across three sampled depth: 77 m (A); 200 m (B); 244 m (C). ....	25
Figure 13: Biovolume of <i>Beggiatoaceae</i> filaments across three stations with water depths of 77 m (A), 200 m (B) and 244 m (C). ....	26
Figure 14: Concentrations of $P_i$ -equiv. stored as polyP in <i>Beggiatoa</i> filaments present in one $cm^3$ sediment. ....	26

Figure 15: “The distributions of $^{18}\text{O}$ and P are shown for the physiological most distinguishable incubation conditions. (A) Optimal growth condition (oxic, low sulfide); (B) stressful condition (anoxic, high sulfide flux). $^{18}\text{O}$ enrichments in atom% are presented in the top panels, and phosphorus content normalized to carbon is presented in the bottom panels with two exemplary ROIs for both polyP (yellow regions) and cytoplasm (white regions), defined by manual assignment” (Langer et al., 2018) .....	27
Figure 16: “C/P ratios, indicative of P content, plotted against $^{18}\text{O}$ enrichments for all determined ROIs. Decreased C/P ratios (high P content) are apparent in areas defined as polyP compared to regions defined as cytoplasm, especially under high sulfide condition” (Langer et al., 2018). .....	28
Figure 17: P (upper panel) and $^{18}\text{O}$ (lower panel) distribution in filaments which were exposed to low sulfide fluxes and incubated under oxic (A), anoxic (B), and cooled (= control, C) conditions.....	29
Figure 18: P (upper panel) and $^{18}\text{O}$ (lower panel) distribution in filaments which were exposed to high sulfide fluxes and incubated under oxic (A), anoxic (B), and cooled (= control, C) conditions.....	30
Figure 19: “Boxplots from ROIs based on P counts for different treatments (oxic, anoxic, control) during low sulfide flux (A) and high sulfide flux (B). Different letters indicate boxes that differ significantly between treatments exposed to the same sulfide fluxes ( $P < 0.05$ ). Boxes with same letters are not significantly different ( $P > 0.05$ ). The asterisk indicates the box being significantly different between different sulfide concentrations within the same treatment. The horizontal line at 0.2 atom% presents the natural abundance of $^{18}\text{O}$ ” (Langer et al., 2018). .....	31
Figure 20: Sulfur counts in low sulfide treatments for Control (A), Oxic (B) and Anoxic (C) incubations. ....	34
Figure 21: Sulfur counts in high sulfide treatments for Control (A), Oxic (B) and Anoxic (C) incubations. ....	35
Figure 22: Upper panels: nanoSIMS counts of P signals in four different filaments after 24 h ex situ incubation with $^{18}\text{O}$ -water. Lower panels: $^{18}\text{O}$ enrichments in P rich spots (green) and P poor spots (orange). $^{18}\text{O}$ enrichments in ROIs defined as polyP were significantly higher than ROIs defined as Cytoplasm in filaments A + B. ....	36
Figure 23: Current understanding of polyP cycling in sediments. A: $\text{P}_i$ uptake and the formation of polyP during oxic conditions; B: polyP degradation and $\text{P}_i$ release into the extracellular environment during anoxic conditions.....	45
Figure 24: Phosphate fluxes across the Peruvian shelf (Lomnitz et al., unpublished).....	46
Figure 25: Hypothesized effect of enzyme mediated oxygen isotopes exchange when incubated with $^{18}\text{O}$ -labelled water. $^{18}\text{O}$ enrichments in polyP above the natural abundance of 0.2% is attributed to enzymatic activity.....	49

Figure 26: Conceptual model showing one possible way for  $^{18}\text{O}$  labeling of polyP. A: Oxygen is initially present as  $^{16}\text{O}$ , both in water and  $\text{P}_i$ /polyP. B: After the addition of highly labelled  $^{18}\text{O}$  water to the *Beggiatoa* mat, labelled water diffuses into the cytoplasm. C: Activity of PPase leads to a fully exchange of oxygen atoms in  $\text{P}_i$ . D: PPK adds  $^{18}\text{O}$  labelled  $\text{P}_i$  to polyP chains leading to  $^{18}\text{O}$  enrichments in polyP. .... 50

---

**List of Tables**

Table 1: Conditions during 24 h incubation of <i>Beggiatoa</i> filaments with <sup>18</sup> O- water. ....	17
Table 2: Minimum and maximum <sup>18</sup> O enrichments [atom%] for ROIs defined as polyP.....	32
Table 3: Minimum and maximum <sup>18</sup> O enrichments [atom%] for ROIs defined as cytoplasm. ....	33
Table 4: “Mean values of <sup>18</sup> O enrichments in ROIs defined as polyP and as cytoplasm and the ratio between the means of enrichments in polyP and cytoplasm. It becomes evident that the ratio is distinctively higher in treatments exposed to high sulfide fluxes, both under oxic and under anoxic conditions” (Langer et al., 2018).....	33
Table 5: In situ bottom water oxygen concentrations during sediment sampling (Data: Clemens et al., unpublished) .....	41
Table 6: Maximum relative contribution of <i>Beggiatoa</i> filaments to measured in situ P <sub>i</sub> release and time until the polyP pool would be depleted if not continuously regenerated. Calculation with P <sub>i</sub> fluxes from Figure 24 (3500 μmol*m <sup>-2</sup> *d <sup>-1</sup> in 77 m; 250 μmol*m <sup>-2</sup> *d <sup>-1</sup> in 200 m and 244 m).....	47
Table 7: Expected <sup>18</sup> O enrichment in polyP with PPX as the dominate enzyme leading to exclusively <sup>18</sup> O enriched terminal P <sub>i</sub> residues.....	51

## Acknowledgment

The time I spend working on and writing up this thesis was accompanied by several people.

Therefore I want to thank...

...first of all Prof. Dr. Heide Schulz-Vogt for all the support in the last years, the always open doors and the honest and open discussions.

...all members of the working group for the nice working atmosphere and especially Christin for all the indispensable help when needed.

...Dr. Angela Vogts for nanoSIMS measurements and the support with data analysis.

...the Geomar people making my participation at the M137 cruise possible.

...the Baltic Transcoast students for often constructive talks and Julia, Matthias and Xaver for the all in all enjoyable time in our small office.

...many other IOW PhDs for the regular coffee meetings providing new energy for writing

...last but not least my family for all the moral support and always believing in me. This is especially true for Maria - thank you for everything and all the time we spend together.



## **Declaration of Authorship**

I hereby declare that this thesis was written by my own and that I have not used any other sources than marked and acknowledged as references. All figures and tables were prepared by me if not labelled otherwise. I further confirm that this thesis was not submitted before at any other institution.

Simon Langer

Rostock, 23.08.2019